All-electron local-density theory of alkali-metal bonding on transition-metal surfaces: Cs on W(001)

E. Wimmer* and A. J. Freeman
Materials Research Center and Physics Department, Northwestern University, Evanston, Illinois 60201

J. R. Hiskes and A. M. Karo
Lawrence Livermore National Laboratory, Livermore, California 94550

(Received 3 January 1983)

A theoretical study of the nature and the mechanism of the bonding of an alkali metal (Cs) on a transition-metal surface [W(001)] in the high-coverage limit is presented in order to understand and explain the lowering of the work function and to elucidate the role of W surface states and surface resonance states in the adsorption process. The analysis is based on all-electron local-density–functional results obtained with our self-consistent full-potential linearized augmented-plane-wave method for thin films for (1) a five-layer slab of W, (2) an unsupported Cs monolayer, and (3) Cs in a $c(2\times2)$ structure on both sides of the five-layer W slab for three different Cs-W separations. We find that Cs forms a polarized-metallic rather than ionic overlayer: The Cs valence electrons originating from the atomic 6*s* states are polarized toward the W surface leading to an increase of electronic charge in the Cs/W interface region and a depletion of electronic charge on the vacuum side of the overlayer. In addition, the semicore Cs 5*p* electrons are markedly counterpolarized. The net result of these multiple surface dipoles is a lowering of the work function upon cesiation from 4.77 eV (clean five-layer W slab) to 2.77, 2.55, and 2.28 eV, corresponding to heights of the Cs atoms above the W surface of 2.60, 2.75, and 2.90 Å, respectively. The Cs-induced changes in the charge density are essentially localized outside the surface W atoms. The W *d* surface states and surface resonance states which are so characteristic of the W(001) surface are found to persist on the cesiated W(001) surface. The main effect of the Cs overlayer on these states is their energetic stabilization; this effect is most pronounced for the contamination-sensitive $\bar{\Gamma}_1$ surface state just below the Fermi energy, which is lowered in energy by 1 eV due to hybridization with Cs *s* states.

I. INTRODUCTION

In their pioneering work Kingdon and Langmuir[1] discovered that the electron emission rate of a tungsten surface was greatly enhanced by the deposition of a Cs overlayer. Furthermore, they found that Cs atoms striking a hot W surface were backscattered as positive ions. Subsequently Becker[2] found that the electron emission rate of a cesiated tungsten surface was even larger in the presence of coadsorbed oxygen. These classic effects of work-function lowering and ionic desorption play the key role in technical applications of the Cs/W system such as photoemitters,[3] secondary electron emitters, thermionic emitters, thermionic energy conversion,[4] ion propulsion systems,[5] and play a decisive role in H^- and D^- negative-ion sources for magnetic fusion energy neutral-beam devices.[6–8]

This variety of technical applications was supported by a continuing experimental and theoretical effort for a deeper understanding of the Cs/W system. Early experiments on Cs/W polycrystalline samples employed mainly desorption techniques to study mobilities,[9] coverages, and desorption rates as a function of temperature and pressure.[9,10] Taylor and Langmuir[10] found that the binding energy of Cs decreased with increased coverage from 2.83 eV per atom at low coverage to 1.77 eV per atom at monolayer coverage. They established a minimum in the electronic work function of 1.70 eV connected with a maximum in the electron emission rate before reaching complete monolayer coverage. Field-electron–microscopy studies of Cs on W (Refs. 11 and 12) shed light on the nature of the adsorbed state: Utsugi and Gomer[11] explained their data by assuming a polar rather than ionic ground state for Cs on W, very similar to Ba on W (Ref. 13) and K on W (Ref. 14). The polarizability of adsorbed Cs was found to be very close to that of the free atom.[11] In the past two decades the low-energy electron diffraction (LEED) technique brought a detailed understanding of the structure of Cs on single-crystal faces of W. MacRae *et al.*[15,16] observed for increasing Cs coverage on a W(001) surface a $c(2\times2)$, then a $p(2\times2)$, and finally a hexagonal LEED pattern and found the minimum of the work function to coincide with the $p(2\times2)$ overlayer structure. MacRae *et al.* associated the $c(2\times2)$ structure with an ionic Cs monolayer and attributed the subsequent $p(2\times2)$ and the hexagonal structures to a second Cs layer. This duolayer model has been criticized by Fehrs *et al.*[17] since it leads to a very high Cs coverage at the work-function minimum in disagreement with other measurements.[18] Voronin *et al.*[19] suspected that the $c(2\times2)$ LEED pattern observed by MacRae *et al.* could be due to residual gases and suggested that the minimum of the work function corresponds to the first Cs layer. Papageorgopoulos and Chen[20] showed in a LEED study of the coadsorption of

Cs and H_2 on W(001) that indeed small amounts of Cs caused the formation of ordered hydrogen patches in a $c(2\times2)$ structure. Thus it is now accepted that the minimum of the work function in the Cs/W(001) system occurs at a Cs coverage of one Cs atom for four W atoms with Cs forming an ordered $p(2\times2)$ overlayer. At a saturated Cs layer the value of the work function reaches a plateau. The values in eV for the work function at the minimum (plateau) are given as $1.60\pm0.05(1.76\pm0.05)$,[12] 1.58(1.78),[20] and 1.58(1.80).[21] Cesium and oxygen also mutually influence their surface structures on the W(001),[22] (112),[23,24] and (110) (Refs. 25 and 26) faces. It is interesting to note that for the system Cs/O/W(001) the maximum photoemission efficiency is reported[27] to be near (coverage $\Theta=0.29\pm0.03$ corresponding to 2.9×10^{14} Cs atoms per cm^2) but not at the work-function minimum (coverage $\Theta=0.25$). Improvements in field emission and field desorption techniques made a measurement of binding energies and dipole moments of single alkali-metal atoms on W surfaces accessible.[28] Todd and Rhodin[28] report a binding energy per Cs atom on W(110), (112), and (111) of 3.06 ± 0.05, 2.66 ± 0.04, and 2.30 ± 0.05 eV, respectively, which compares to 2.80 eV for W(100) (Ref. 29) extrapolated to the dilute limit. Studies using reflection high-energy electron diffraction (RHEED) and Auger electron spectra (AES) (Ref. 30) have exhibited a metastable registered Cs phase on W(100) at 0.81 ± 0.03 ML before a hexagonal overlayer is formed at monolayer saturation (equal to 1 ML) where the nearest-neighbor distance is about 11% less than in bulk Cs metal. Recently, the visualization of adsorbed submonolayers of Cs on polycrystalline W has become possible by scanning-electron-microscope (SEM) techniques.[31]

This wealth of experimental data has stimulated a variety of theoretical models and approaches to describe the alkali-metal adsorption on metal surfaces. After the discovery of the work-function lowering and the desorption of positive Cs ions, Langmuir[32–34] proposed the following model: Cs is adsorbed on W in the form of a positive ion giving one electron to the substrate. The Cs^+ ion and its negative-image charge form a dipole that reduces the work function of the surface. At higher coverages the interaction between the dipoles reduces the effective dipole moment per adatom, the work function goes through a minimum and increases from there on to the high-coverage value. This model also explains the decrease of binding energy—seen as the force between the ion and its image—with increased coverage. Langmuir's criterion for Cs to desorb as a neutral atom or as a positive ion was the difference between the first ionization potential of Cs (3.89 eV) and the work function of the surface: At low coverages (which is the case at high temperatures) the work function is larger than 3.89 eV and Cs desorbs ionically. Gurney[35] criticized this ionic picture of alkali-metal adsorption by pointing out that barium also reduces the work function of tungsten yet its first ionization potential is greater than the W work function. He was one of the first to stress the fact that the adsorption of an atom on a surface should be treated quantum mechanically considering the system of the adsorbed atom and the substrate as an entity. Gurney showed in a simple quantum-mechanical model that the valence level of an atom is broadened into a band as it approaches the surface. Despite this critique, the classical model of Langmuir has been further developed[36–42] and successfully applied to a phenomenological treatment of the thermodynamic properties of the alkali-metal surface system. The classical picture has been extended even to the point of assuming two distinct adsorbed species (ionic and neutral) coexisting on the surface.[39,43–46] Other workers[47–54] proposed a model in which the adsorbed particles exist only as a single species bound to the surface by polarized or partially ionic and partially covalent bonds. Based on this model (which emphasizes the local aspects of the adsorbate-substrate bonding) semiempirical calculations have been performed for desorption energies.[54–56]

The need for a realistic and rigorous quantum-mechanical treatment of the alkali-metal adsorption problem was strongly felt as early as the 1930s.[35] But even 30 years later this goal seemed to be out of reach. So, for example, Levine and Gyftopoulos[54] state the ideal approach to the problem of calculation of desorption energies would be to treat the chemical surface bond quantum mechanically. This is, however, an extremely difficult task. As a consequence the problem has been approached semiempirically[48–54] or by using a simplified Hamiltonian.[57–76] In particular the Anderson impurity approach proved to be an interesting starting point[77,78] for treating the atomic adsorption at low coverages.[58–67] It is interesting to note that Bennett and Falicov[58] find for K on W at small distances "true metallic character." A simple model for the adsorption process is obtained by replacing the metal surface by a semi-infinite jellium and studying the electronic structure of atoms as they approach the jellium edge. This approach became particularly popular[68–73] when density-functional theory[79,80] provided an elegant framework for dealing with the many-body problem. A simple but nevertheless surprisingly successful model has been suggested by Lang,[74] who replaced the adsorbate overlayer by a jellium slab. For this system Lang solved the local-density–functional problem self-consistently and showed that this model was capable of describing the characteristic minimum in the work function versus coverage curve. This encouraged further use of the model.[75,76] A pioneering attempt at a quantum-mechanical treatment of the alkali-metal adsorption problem in terms of an atomistic approach has been reported by Wojciechowski[81,82] who employed a linear combination of atomic orbitals (LCAO) basis using a configuration-interaction technique. For a more detailed and complete discussion of the different approaches to the alkalki-metal adsorption problem the reader is referred to a number of review articles.[83–88]

All the theoretical approaches to the alkali-metal adsorption problem discussed above have in common the feature that they do not attempt an all-electron treatment which incorporates the full atomistic aspect of the system, since the task seemed monumental. In the past decade it became more and more evident that the local approximation to the density-functional theory[79,80] gave a consistently accurate and realistic description of the electronic structure and the energetics of condensed[89,90] and also molecular[91] systems. This fact has stimulated the development of

methods which allow local-density calculations for surfaces and surfaces with adsorbed atoms including the atomistic nature of the surface.[92–95] One of the most accurate and efficient theoretical and computational approaches for condensed systems is the linearized–augmented–plane-wave (LAPW) method.[96–98] In recent years this LAPW method, originally designed for bulk systems has been adapted for a film geometry.[99–101] It has been demonstrated that this single-slab geometry provides a promising approach to the theoretical and computational treatment of the electronic structure of clean surfaces[100–103] and surfaces with overlayers.[104–106]

Because of the reduced symmetry and reduced coordination number of atoms at a surface, a realistic quantum-mechanical treatment has to allow for a general charge density and potential, since shape (such as muffin-tin) approximations not only could influence the results in an uncontrolled way but would also cloud the strengths and limits of the local-density approach to density-functional theory. Recently, we have presented the full-potential linearized–augmented–plane-wave (FLAPW) method for thin films[107] in which no shape approximations are made to the density and the potential, hence solving the local-density–functional (LDF) one-particle equations fully self-consistently. We present here the results of an all-electron study of the electronic structure of a Cs overlayer on a W(001) surface using this highly accurate all-electron FLAPW method.[108] Section II describes briefly the theoretical approach and methodology. Results for the surface states and surface resonance states are given in Sec. III, charge densities in Sec. IV, and work-function lowering and core-level shifts in Sec. V. A summary and conclusion is presented in Sec. VI.

II. METHODOLOGY AND THEORETICAL AND/OR COMPUTATIONAL ASPECTS

It is now generally accepted[19,20] that with increasing Cs coverage of an unreconstructed W(001) surface the first-ordered Cs structure is a $p(2\times2)$ coverage with Cs atoms in fourfold hollow sites. For this coverage (one Cs atom for every group of four W atoms, coverage $\Theta=0.25$) the Cs/W(001) system has its minimum of the work function. As a completed monolayer coverage, Cs forms a hexagonal overlayer. Voronin *et al.*[19] suggest a distorted hexagonal commensurate structure with the Cs atoms in bridge position (coverage $\Theta=0.50$) whereas Papageorgopoulos and Chen[20] propose a close-packed structure with coverage $\Theta=0.43$. No experimental results for the height of the Cs atoms are known to the authors. Yet this height is crucial for the theoretical value of the work function. A calculation of the $p(2\times2)$ structure using a five-layer W(001) slab as a substrate would result in a unit cell of 22 atoms, an almost overwhelming number for an *ab initio* band-structure calculation. We, therefore, decided to investigate the mechanism of the work-function lowering and the dependence of the work function on the height of the Cs atoms for a $c(2\times2)$ overlayer structure which corresponds in coverage essentially to the completed monolayer (coverage $\Theta=0.50$). This results in a unit cell with 12 atoms, which is still considerable for an *ab initio* film calculation. In our $c(2\times2)$ structure the adsorption site is the same as in the $p(2\times2)$ structure which we plan to tackle in a future step using our $c(2\times2)$ results as a starting point.

We have carried out independent all-electron self-consistent local-density–functional energy-band studies of three systems: (i) a five-layer slab of W(001), (ii) an unsupported monolayer of Cs, and (iii) Cs in a $c(2\times2)$ overlayer on both sides of the W(001) five-layer slab (12 atoms per film unit cell). We have performed self-consistent calculations for three heights ($d=2.60$, 2.85, and 2.90 Å) of the Cs atoms. The clean W(001) surface is represented by a single slab of five layers where all W-W distances correspond to the bulk lattice parameter $a_0=5.973$ a.u. The square lattice of the Cs monolayer is assumed to have the same Cs-Cs distances as a $c(2\times2)$ Cs overlayer on a W(001) surface, i.e., $\sqrt{2}\times5.973$ a.u. The cesiated W surface is described as a five-layer slab of W with Cs on both sides in the form of a $c(2\times2)$ overlayer in fourfold hollow sites (cf. Fig. 1), i.e., one Cs atom to two surface W atoms. We employ the Wigner exchange-correlation potential[109] given by $V_{xc}=-1.969\,490\,044t-t(1.888+17.8t)/(1+12.57t)^2$ with $t=\rho^{1/3}$ in the local-density–functional one-particle equations. These equations are solved self-consistently by our FLAPW method for thin films.[107] The main features of this FLAPW method can be highlighted as follows: (i) The variational basis set used in the FLAPW method is one of the most flexible and accurate known today for periodic systems[107,110,111] and its convergence can be monitored easily and systematically in contrast to LCAO-like basis sets. (ii) The charge density and the effective potential are ex-

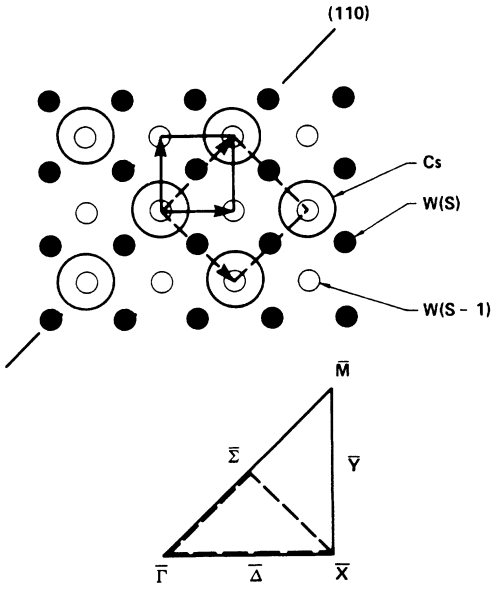

FIG. 1. Structure of $c(2\times2)$ Cs on W(001). The unit cell of the clean (solid lines) and cesiated (dashed lines) surface are rotated by 45° relative to each other. Shown below is the irreducible wedge of the first Brillouin zone for the clean (001) surface (solid lines) and for the $c(2\times2)$ structure on the (001) surface (dashed lines).

panded in Fourier series outside and in spherical harmonics inside the atomic spheres. Thus the choice of geometrical parameters (such as muffin-tin radii) are chosen merely according to mathematical convenience and have no effect on the physical results, such as eigenvalues and charge densities. (iii) Poisson's equation is solved for a full potential (i.e., no shape approximations) using our recently developed technique which goes beyond Ewald-type methods.[107,112] (iv) The core is recalculated in each iteration fully relativistically and all relativistic effects except spin-orbit splitting are taken into account for the valence electrons. (v) The convergence in iterating to self-consistency is accelerated by an extrapolation algorithm of Anderson[113] as pointed out by Hamann.[114]

For each of the 19 $\vec{k}$ points in the irreducible wedge of the two-dimensional Brillouin zone, the wave functions are expanded in about 2×450 linearized augmented plane waves (the mirror symmetry in the center plane of the film is explicitly used to construct even and odd wave functions). The expansions in spherical harmonics inside the spheres for the wave functions, the charge density, and the potential are taken up to $l=8$. The rms value for the fitting in the exchange potential in the interstitial region was about 2.5 mRy, about 0.1 mRy inside the spheres near the sphere boundary, and of the order of 10^{-5} mRy in the interior of the spheres. Self-consistency was assumed when the input and output potentials had an rms deviation of less than 3 mRy. By then the eigenvalues were converged to about 0.3 mRy.

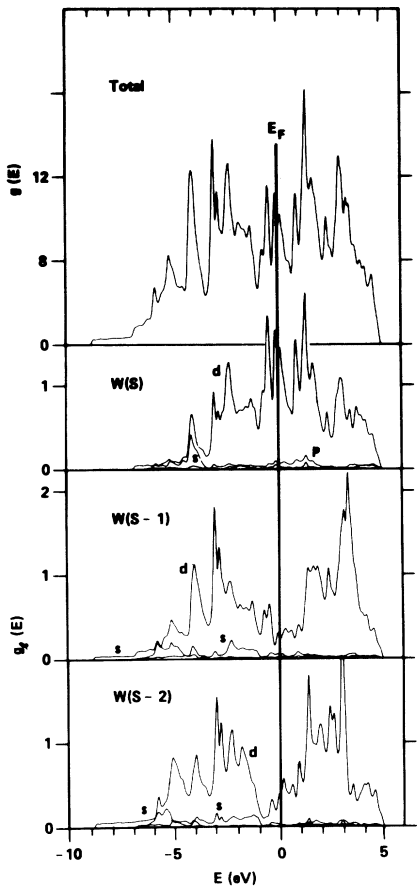

FIG. 2. Total and partial (i.e., atomic layer and l-projected) densities of states for a clean five-layer W(001) film (in states/eV unit cell) which contains 30 valence electrons. S denotes atoms in the surface layer, $S-1$ and $S-2$ label atoms one and two layers below the surface.

III. SURFACE STATES AND SURFACE RESONANCE STATES

One of the most striking electronic features of the W(001) surface are its surface states and surface resonance states.[101,115–117] Hence we discuss in this section the local-density–functional single-particle energy spectrum in its $\vec{k}$-resolved form (i.e., the energy-band structure) and its $\vec{k}$-integrated form [i.e., the density of states (DOS)]. The decomposition into atomic and l-projected densities of states for the clean W(001) slab (cf. Fig. 2) shows that two layers below the surface (S-2) we find the characteristic features of a bulk bcc transition metal: A flat sp-like DOS and a sharp d-like DOS with a characteristic minimum which occurs for W (six valence electrons) just below the Fermi energy. The surface-projected DOS (Fig. 2) shows states just below the Fermi energy where the bulklike DOS has its pronounced minimum. These states, which are also clearly visible in the total DOS (Fig. 2), are known as surface states (SS) and surface resonance (SR) states[101] and are expected to be influenced by overlayers. For a more detailed picture we now focus on the most characteristic part of the $\vec{k}$-resolved one-particle energy spectrum of the W(001) surface, namely the band structure along the $\bar{\Gamma}$-$\bar{M}$ symmetry line[116] which is shown in Fig. 3 for the clean five-layer W(001) slab. The black area in the circles gives the relative surface character. Our results agree with those of Krakauer *et al.*[102] and Posternak *et al.*,[101] who applied their warped muffin-tin LAPW method to seven-layer W(001) films: At $\bar{\Gamma}$ we find a localized SS just below the Fermi energy. Two SR bands, one of $\bar{\Sigma}_2$ symmetry [Fig. 3(a)] and one of $\bar{\Sigma}_2$ symmetry [Fig. 3(b)], are found to cross the Fermi energy at about $(\frac{5}{8},\frac{5}{8})\pi/a$. Note that each of these bands is split into a pair of even $(+)$ and odd $(-)$ symmetry with respect to mirror reflection at the center plane of the film. This splitting originates from residual interactions of the two surfaces of the five-layer film. Another SS band found at $\bar{\Gamma}$ at about -0.7 Ry gradually loses its surface character away from $\bar{\Gamma}$. Near $\bar{M}$ we observe a rather complicated structure of surface states with a relative surface character of only 50%. The pair of bands $\bar{\Sigma}_1(+),\bar{\Sigma}_2(-)$ and $\bar{\Sigma}_1(+),\bar{\Sigma}_2(-)$ of SR states near E_F and, as reference, the adjacent lower-lying bands [cf. the labeled bands in Figs. 3(a) and 3(b)] have been selected from the band structure of the clean W(001) surface and backfolded into the first Brillouin zone of the cesiated surface [left-hand sides of Figs. 4(a) and 4(b)]. Now the effect of the cesiation on these states can be studied by comparing with the corresponding energy bands of $c(2\times2)$ Cs on W(001) [right-hand sides of Figs. 4(a) and 4(b)]. For convenience the eigenvalues are shifted to the same Fermi energy. The most striking result from this

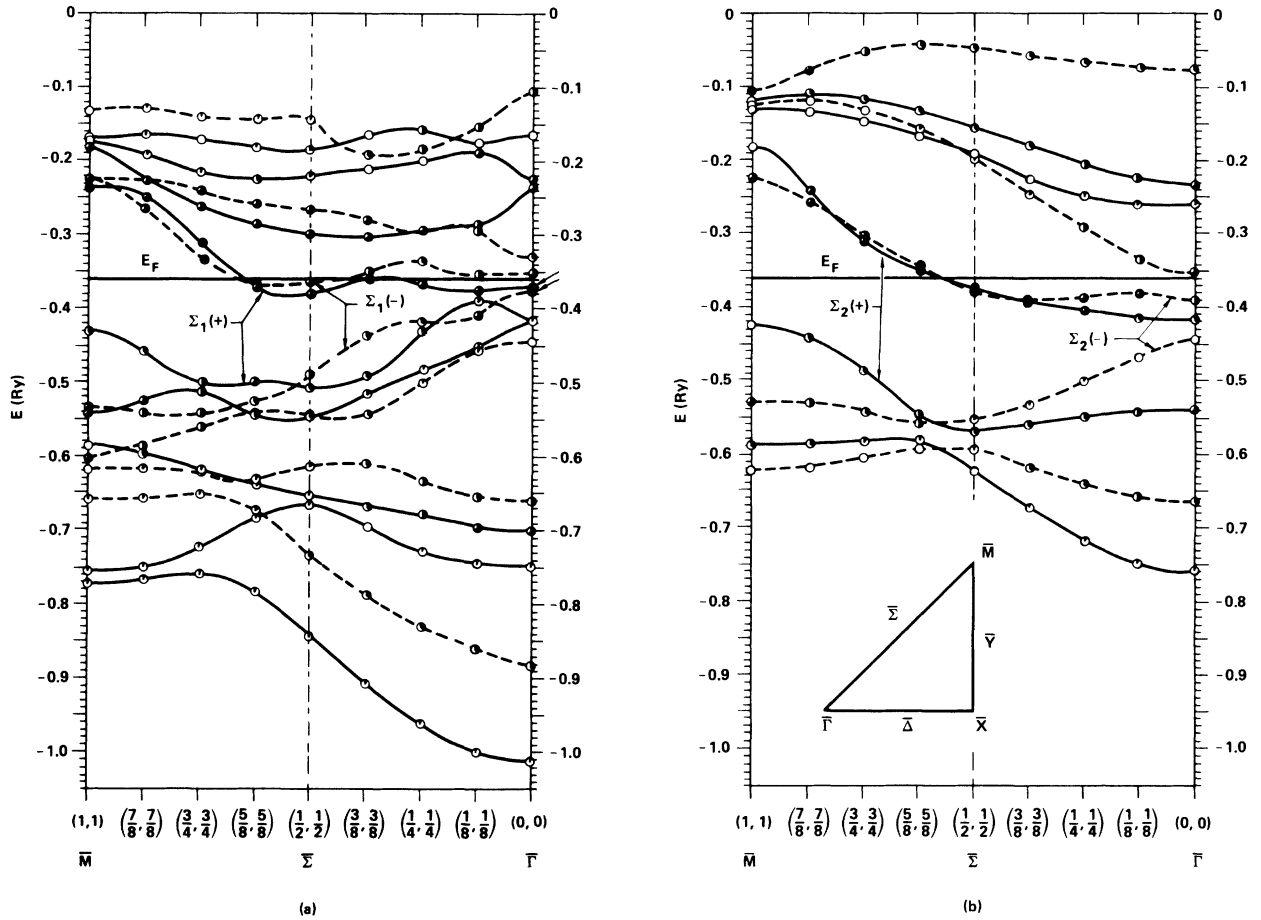

FIG. 3. Energy-band structure of a five-layer W(001) film: States along $\bar{\Gamma}-\bar{M}$ with (a) even and (b) odd symmetry with respect to a mirror reflection on the (110) plane. Solid (dashed) lines denote states which are even (odd) with respect to z reflection on the center plane. $\vec{k}$ is given in units of π/a with $a=5.973$ a.u. The black area within the circles indicates the relative surface character of a state. The pair of contamination sensitive surface states with $\bar{\Gamma}_1(+)$ and $\bar{\Gamma}_1(-)$ symmetry is indicated by arrows. The inset shows the irreducible wedge of the two-dimensional Brillouin zone.

comparison is that the $\bar{\Gamma}$ SS just below E_F [marked by arrows in Fig. 4(a)] is lowered in energy by 1 eV upon cesiation. The SR bands near the Fermi energy are also found to be shifted to larger binding energies but to a lesser extent. The lower bands, which have been selected as a reference, are hardly affected by the cesiation as can be seen from Figs. 4(a) and 4(b).

We now focus just on the eigenvalues at $\bar{\Gamma}$ near the Fermi energy and compare the states of the clean five-layer W(001) slab, the Cs monolayer, and of the cesiated W surface for three different heights of the Cs atoms, all shifted to the same Fermi energy. Furthermore, we classify the states according to their atomic (i.e., layer) and l-projected character. The most striking observation (Fig. 5) is the interaction between W d SS and the Cs s conduction band which brings about the dramatic lowering in energy of the $\bar{\Gamma}_1$ SS. In the unoccupied part of the energy spectrum we find interaction of Cs p- and d-like states with the W d SS. As expected, the energies of these hybridized states show a pronounced dependence on the Cs-W separation.

The stabilization of W d states at the surface, which we have discussed so far in terms of characteristic parts of the energy-band structure, is found consequently also in the total densities of states (Fig. 6): The general structure and peak positions of the occupied states for the cesiated W surface resemble very closely those of the clean W surface. The SS and SR states just below E_F are indeed found to be shifted slightly to lower energies (see the arrows in Fig. 6) but without changing their intensity too much. Owing to the unoccupied Cs p- and d-like states, the density of states above E_F is changed markedly upon cesiation. Essentially, we find a higher density of states at about 1 eV above E_F in the cesiated surface as compared to the clean surface. The sharp peak near -10 eV originates from the Cs $5p$ semicore states and almost overlaps with the bottom of the W valence band. The states between -9 and -7 eV have mainly free-electron-like character (compare with the l-projected DOS of Fig. 2). In the Cs monolayer, the $5p$ semicore states are crystal field split into lower-lying p_z-like and (at about 0.2 eV higher) p_x,p_y-like states (see the structure at -11 eV for the Cs monolayer in Fig. 6). As the Cs overlayer is brought close

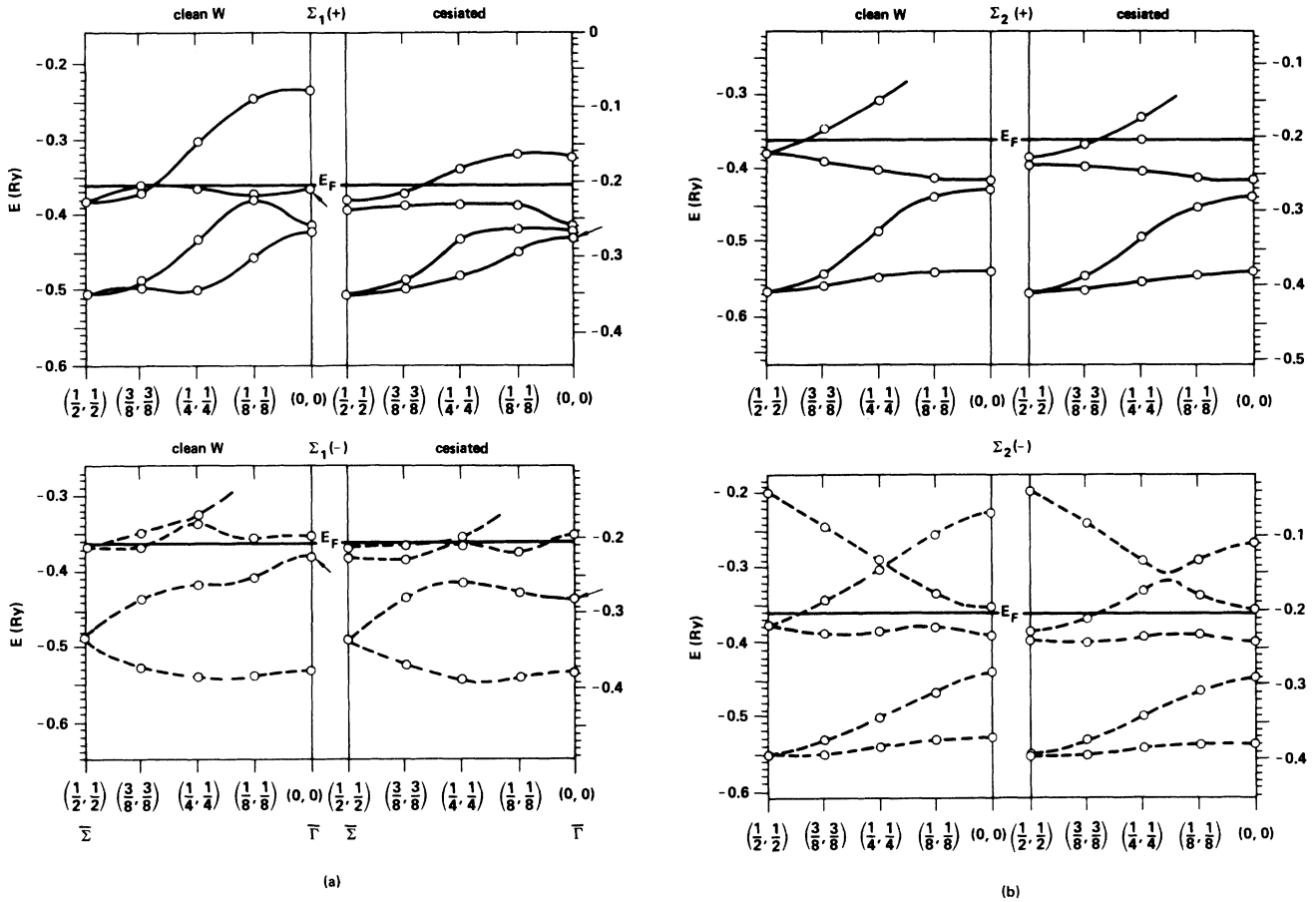

FIG. 4. Selected bands of the clean W(001) five-layer slab (labeled bands in Fig. 3) backfolded to the Brillouin zone of the cesiated W(001) surface and the corresponding bands of the cesiated W(001) surface ($d = 2.60$ Å) for even (a) and odd (b) states with respect to a mirror reflection on the (110) plane. Solid (dashed) lines indicate states with even (+) and odd (−) symmetry with respect to reflection on the central plane of the film. The adsorption-sensitive pair of surface states $\bar{\Gamma}_1(+)$ and $\bar{\Gamma}_1(-)$ is marked by arrows.

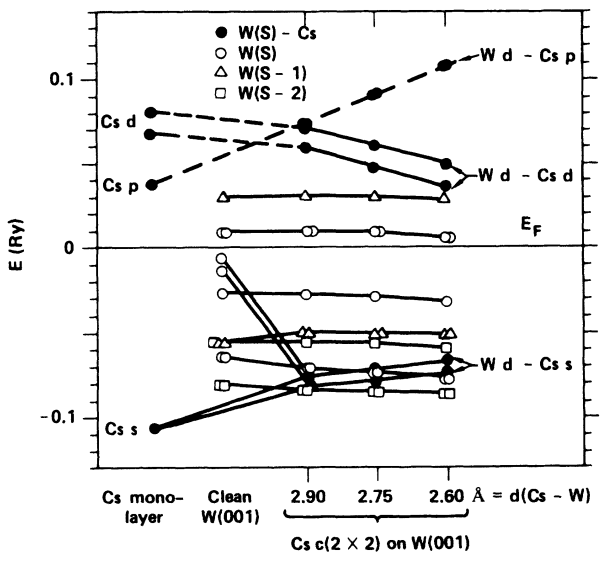

FIG. 5. Atomic (layer) and l-projected character of the states at $\bar{\Gamma}$ for clean W(001), a Cs monolayer, and $c(2\times2)$ Cs on W(001) for three different heights of the Cs atoms. All states are referred to the same Fermi energy. For clean W(001), states from $\bar{M}$ have been backfolded to $\bar{\Gamma}$ (cf. Fig. 1).

to the W surface, the p_z-like states become energetically less favorable compared to the p_x,p_y-like states, and for d(Cs-W)=2.60 Å the p_z-like semicore states can be seen on the higher-energy side of the sharp 5p peak (see bottom panel of Fig. 6).

IV. CHARGE DENSITIES

As stated earlier in terms of one-particle energies, one of the most striking effects of cesiation on the W SS and SR states is the energetic stabilization by 1 eV of the $\bar{\Gamma}$ SS. A study of the one-particle charge density of this state provides further insight into this stabilization mechanism. The $\bar{\Gamma}_1$ SS just below E_F on the clean W(001) surface is known[101] to have mostly $d_{3z^2-r^2}$-like character and projects quite far out into the vacuum (Fig. 7). When Cs is deposited on the W(001) surface, the wave functions of this SS overlap with those of the conduction electrons of Cs (Fig. 8 shows the bottom of the conduction band in a Cs monolayer) to form a new bonding state, which is depicted in Fig. 7. The shape of this Wd—Css hybridized state suggests important polarized-covalent contributions to the bonding mechanism between Cs and the W(001) surface. It is apparent from the one-particle charge-density plots of

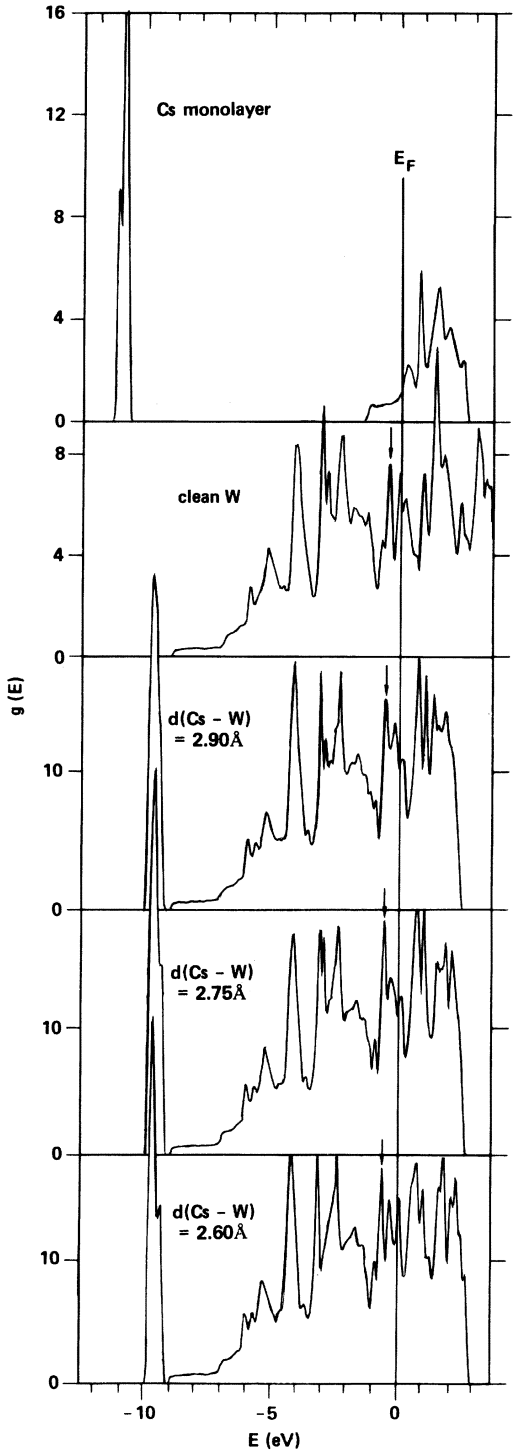

FIG. 6. Total densities of states for a Cs monolayer, a clean five-layer W(001) slab, and $c(2\times2)$ Cs overlayers on both sides of the W slab for d(Cs-W)=2.60, 2.75, and 2.90 Å (in states /eV unit cell) containing 7, 30, and 74 valence electrons, respectively. All Fermi energies have been lined up. Arrows indicate the SS and SR states, which are slightly shifted to higher binding energies upon cesiation.

Figs 7 and 8 that the Cs 6*s* electrons, because of their extended character, lose their identity when Cs is adsorbed on the transition-metal surface and form a new hybridized state. When the wave function of this new state is described by an angular momentum representation near the Cs nucleus, we find that its *s* component has—due to core orthogonalization—a nodal structure which resembles that of an atomic 6*s* function. Despite this resemblance one should consider this state as a new entity, unique to the chemisorbed Cs/W(001) system, and describe it as a hybrid between a W *d* SS and Cs valence state. Thus the energetic stabilization of the $\bar{\Gamma}_1$ SS by 1 eV is explained by the formation of a polarized chemical bond between this surface state and the Cs valence electrons. The energetic stabilization of the other W *d* SS and SR states, which was discussed earlier and found to be less pronounced compared with the $\bar{\Gamma}_1$ SS, indicates similar although weaker bonding mechanisms for these other SS and SR states, which have predominantly d_{xz} and d_{yz} character and project out into the vacuum to a lesser extent.

So far we have focused our attention to states near the Fermi energy. We now consider the charge density of a free-electron-like W state with *sp*-like character at the bottom of the conduction band at $\bar{\Gamma}$ as shown for the clean W(001) five-layer slab in Fig. 9. Besides the sharp nodal structure close to the W nuclei, the charge density of this state has a very gentle modulation inside the film, decays smoothly into the vacuum, and is markedly reduced in the surface layer compared to the center of the film. As noted before, this state lies energetically very close to the Cs 5*p* semicore states (Fig. 6). Therefore, as expected, we find for the cesiated case that the $\bar{\Gamma}_1$ state at the bottom of the W valence band hybridizes with the Cs $5p_z$ states (Fig. 10) indicating that the Cs 5*p* semicore states are involved in the Cs-W interaction. The role of the Cs 5*p* semicore electrons in the cesiation process becomes clearer when we consider the entire valence charge density of the system. The density of states of the Cs/W system (Fig. 6) suggests the splitting of the valence charge density into two parts, one part originating from the energetically isolated "Cs 5*p* band" (between -10 and -9 eV in Fig. 6) and the other part from the occupied "W valence band" (between -9 and 0 eV in Fig. 6). The charge density originating from the Cs 5*p* band is shown in Fig. 11 for the cesiated W(001) surface for three different heights of the Cs atoms (2.90, 2.75, and 2.60 Å) together with the corresponding charge density of an isolated Cs monolayer. The lower panels display the difference between the cesiated W(001) surface and the monolayer. It can be seen that the interaction between the Cs 5*p* electrons and the W substrate increases markedly as the height of the Cs atoms decreases. We observe an increase of charge in the bonding direction between the Cs and surface W atoms, particularly for $d=2.60$ Å. We also notice in the different plots a very pronounced negative region near the Cs nuclei indicating a strong polarization of the Cs 5*p* electrons.

We next discuss the charge density originating from the W valence band. Figure 12 shows in the upper panels to the left the high, localized valence charge density of the clean W(001) surface and to the right the low, extended and weakly bound valence charge density of a Cs monolayer. It becomes immediately obvious that the valence charge density in the surface and interface region is dominated by far by the W *d* states. The three central upper panels in Fig. 12 give the valence-band charge density for

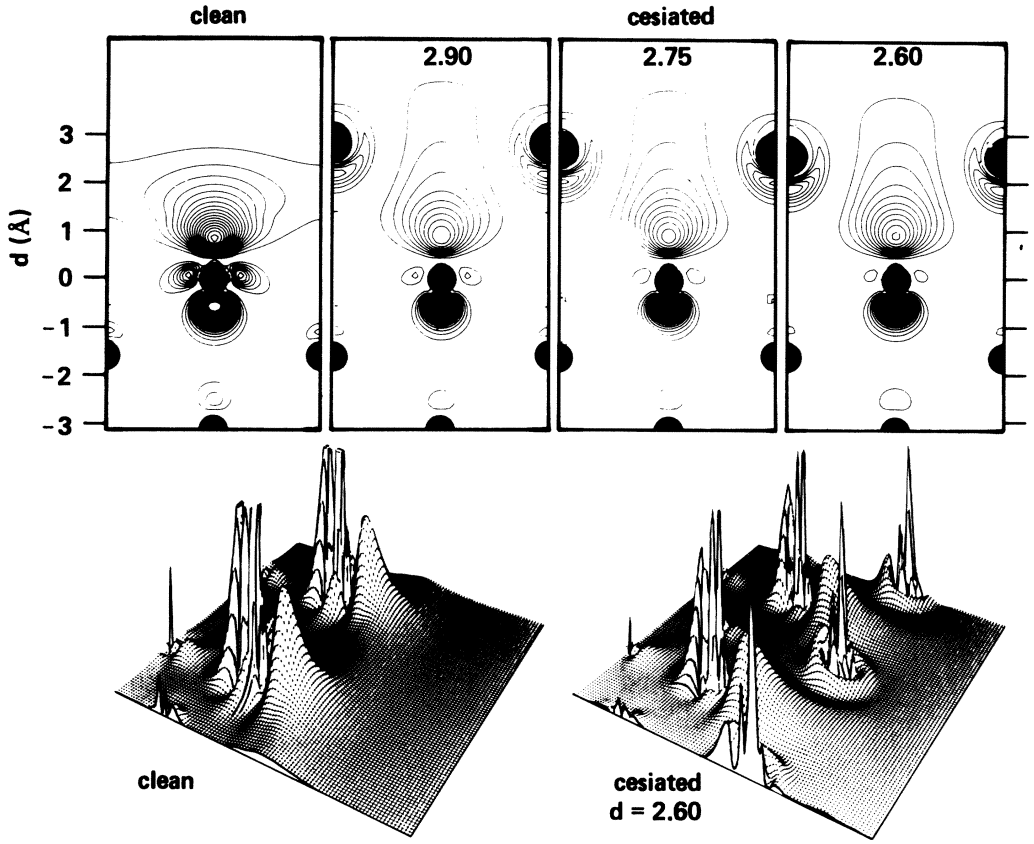

FIG. 7. Single-particle density of the adsorption-sensitive SS $\bar{\Gamma}_1$. The lowest contour and the contour spacings are 0.001 e/bohr^3. In the 3D plots shown below the cutoff is at a density of 0.030 e/bohr^3.

the cesiated W(001) surface. The first surprising observation is the fact that the region near the Cs nuclei *gains* electrons. Thus the quantum-mechanical result clearly contradicts the simple classical picture of a chemisorbed Cs^+ ion. When we compare the charge density inbetween the Cs adatoms for the unsupported Cs monolayer and the chemisorbed Cs (see the contour lines of 1 e/a.u.^{3} in the upper right panel and in the upper central panels of Fig. 12) we observe a polarization of the Cs valence electrons towards the W surface. Clearly, the Cs valence electrons

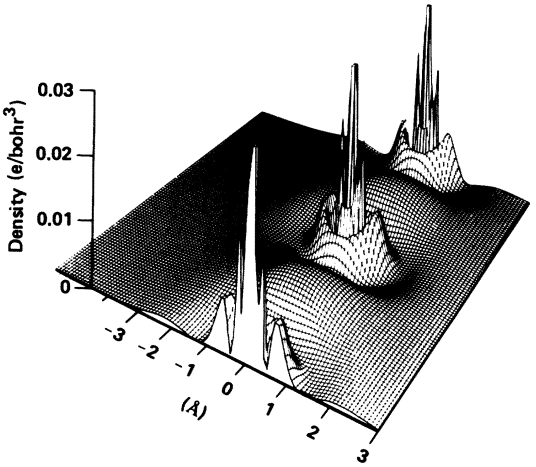

FIG. 8. Single-particle density of the $\bar{\Gamma}_1$ state at the bottom of the conduction band for a Cs monolayer. The density is given in units of e/bohr^3.

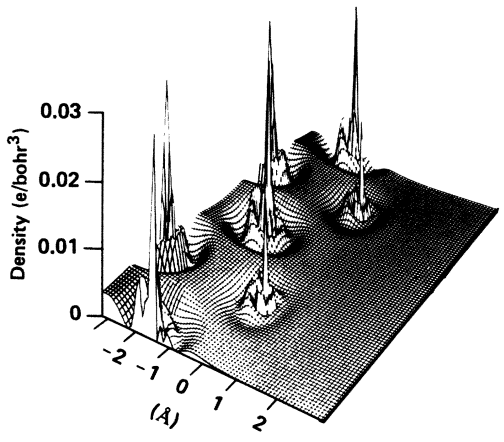

FIG. 9. Single-particle density of the $\bar{\Gamma}_1$ state at the bottom of the conduction band of the clean W(001) five-layer slab in units of e/bohr^3.

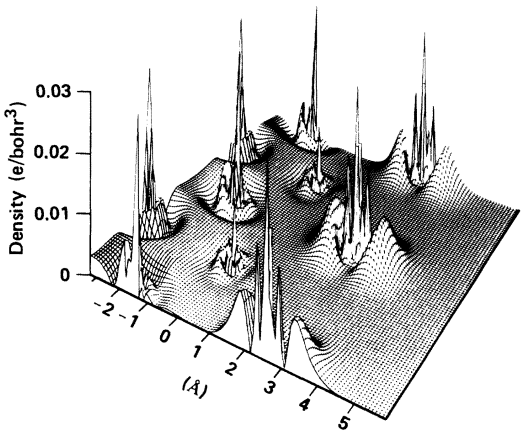

FIG. 10. Single-particle density of the $\bar{\Gamma}_1$ state at the bottom of the W valence band for $c(2\times2)$ Cs on W(001) with d(Cs-W)=2.60 Å. The density units are e/bohr^3.

lose their identity as they penetrate into the high-density region of the W d electrons. From Fig. 12 it also becomes apparent why the region near the Cs nuclei gains electrons: The electrons which spill out into the vacuum on a clean W surface are attracted by the Cs nuclei. The wave functions of these electrons obtain their nodal structure near the Cs nuclei due to the orthogonalization to the Cs core electrons. Clearly, this charge near the Cs nuclei is increased as the Cs atoms are brought close to the surface (Fig. 12). The rearrangement of charge in the valence band is conveniently monitored by the difference between the self-consistent charge and the superposition of the charges from the clean W(001) slab and the Cs monolayer as shown in the lower panels of Fig. 12. As stated, the Cs valence electrons are attracted by the W surface and lead to a depletion of electronic charge between and outside the Cs atoms and to an increase in the interface region. It is remarkable that the charge redistribution takes place essentially *outside* the surface W atoms. Therefore, the classical picture of Cs donating an electron *into* the substrate metal is incorrect. The difference charge-density plots (lower panels of Fig. 12) reveal clearly that the regions near the Cs nuclei show a net gain of electrons of predominantly s- and p_z-like shape.

We are now in a position to discuss the total electronic charge density and its rearrangement upon cesiation (Fig. 13). As described for the valence charge density, the

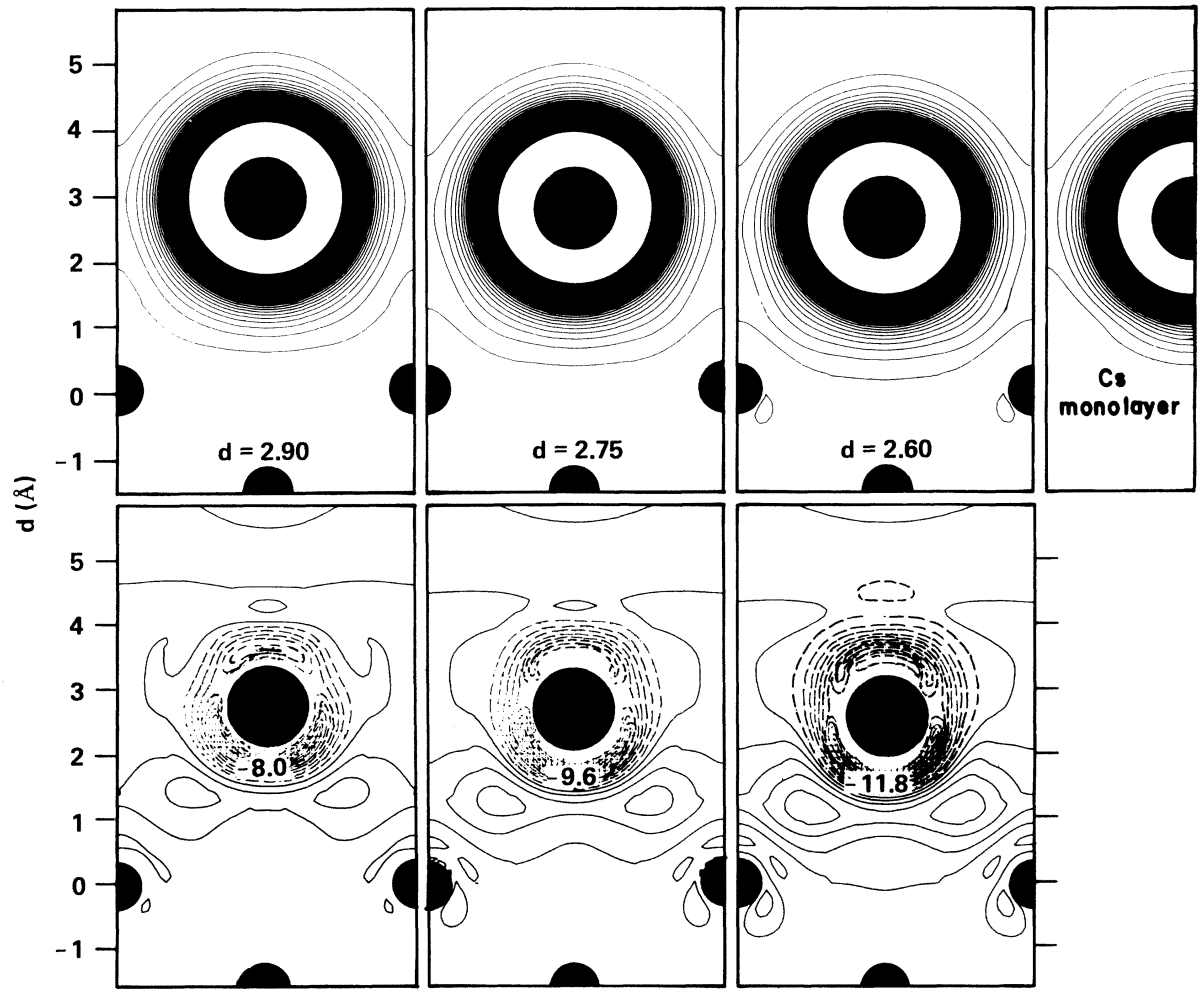

FIG. 11. Upper panels: charge density originating from the Cs 5p band. The lowest contour and the contour spacing are 1×10^{-3} e/bohr^3. Lower panels: the difference ρ_{5p}(Cs/W)$-\rho_{5p}$(Cs monolayer) with a contour spacing of 0.5×10^{-3} e/bohr^3.

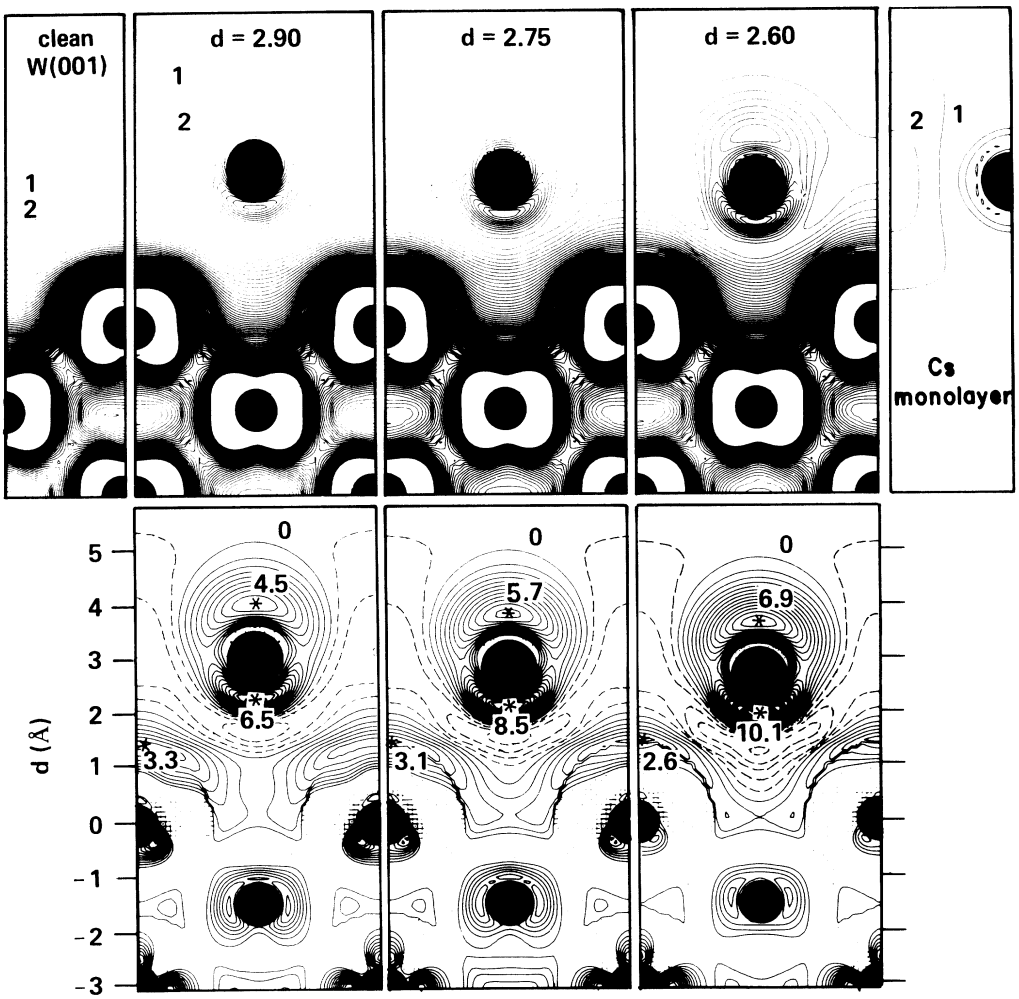

FIG. 12. Upper panels: charge density originating from the W valence band. The lowest contour and the contour spacings are 1×10^{-3} e/bohr^3. The contour plot is cutoff at a density of 75×10^{-3} e/bohr^3. Lower panels: the difference $\rho_{\rm val}$(Cs-W)$-\rho_{\rm val}$(W) with a contour spacing of 0.5×10^{-3} e/bohr^3.

charge redistribution is monitored by the difference between the self-consistent charge density of the cesiated surface and the superposed charge density of the clean W(001) surface and the charge density of a Cs monolayer (lower panels of Fig. 13). As already observed for the valence charge density, the rearrangement of charge takes place mainly in the "interface region," i.e., the region between the planes of the Cs and surface W atoms, and the region outside (the vacuum side) and the Cs atoms. From the regions between and outside the Cs atoms electronic charge is removed and we find an increase of electronic charge in the interface region. This effect can be described as a "polarization of the Cs valence electrons." The charge redistribution near the Cs atoms becomes apparent as a "counterpolarization of the Cs 5p semicore electrons." A simple physical picture emerges from this analysis of the rearrangement of the electronic charge density upon the cesiation of the W(001) surface. The weakly bound, extended, and highly polarizable Cs valence electrons hybridize with the localized, high-density W d electrons of the surface to form a covalent-polarized bond and thus lead to an increase of charge in the interface region and a depletion of charge between and outside the Cs atoms. This creates an extended dipole layer with its negative pole pointing towards the W substrate. Coupled with this "Cs valence polarization dipole" we find a counterpolarization of the Cs 5p semicore electrons producing a smaller dipole with its negative pole pointing towards the vacuum. When the height of the Cs atoms is increased from 2.60 to 2.90 Å these dipoles are found to be strengthened (see lower panels in Fig. 13). In the following section we will discuss the consequences of these Cs-induced dipoles on the electronic work function.

V. WORK-FUNCTION LOWERING AND CORE-LEVEL SHIFTS

As discussed in the Introduction, one of the most striking features of the cesiation of a transition-metal surface is the lowering of the work function. The work function is defined[118] as the difference in energy between a lattice with an equal number of ions and electrons, and the lattice with the same number of ions, but with one electron removed. One of the first and for several decades the most sophisticated quantum-mechanical calculation of the work function was performed by Bardeen.[119] He employed a jellium model for the surface and solved the Hartree-Fock equations for the electron gas ($r_s=4$), including a nonlocal

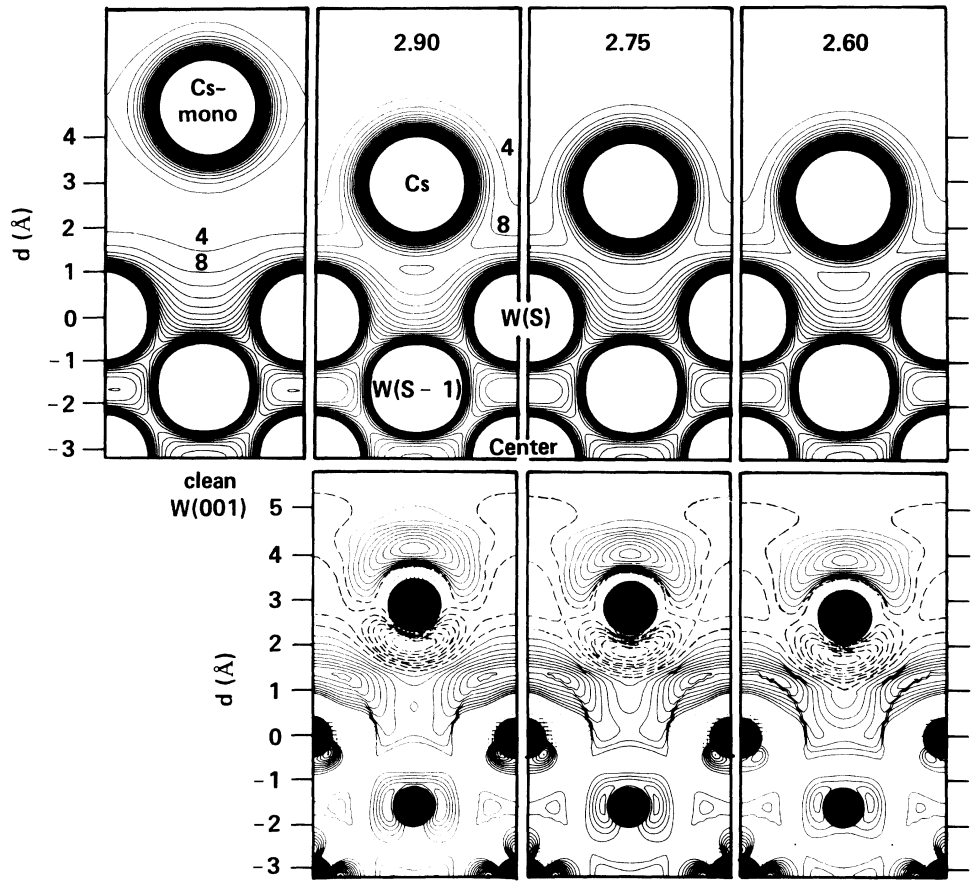

FIG. 13. Upper panels: total electronic density in 10^{-3} e/bohr^3. Lower panels: the difference between the self-consistent density of the cesiated surfaces and the superposed density of a clean W five-layer film and a Cs monolayer.

(energy-dependent) form of the exchange and correlation potential. His results indicate that the surface barrier is due primarily to exchange and polarization forces, and that ordinary electrostatic forces play a minor role. Three decades later, progress in many-body theory led to the formulation of density-functional theory[79,80] which has been subsequently applied to the self-consistent solution of the jellium model for surfaces.[120–122] Using this approach, Smith[121] calculated work functions and surface potentials systematically for a series of metals ranging from low-electron densities (alkali metals) to high densities typical for transition metals. His results confirm that the surface barriers are, in most cases, due to many-body effects, but dipole barriers are found to be small only for alkali metals, and become quite large for the transition metals. The jellium-model calculations have been refined to give surface energies[123] and work functions for different crystal faces by including the effect of the ion cores in a simple pseudopotential theory.[124] The face dependence of the work function has been described earlier by Smoluchowski.[125] Lang and Kohn[124] gave the first rigorous demonstration that the original definition of the work function Φ,[118] as the energy difference between the systems with N and $N-1$ electrons is equivalent to $\Phi=\Delta-\bar{\mu}$, where Δ is the rise in mean electrostatic potential across the metal surface and $\bar{\mu}$ is the bulk chemical potential of the electrons relative to the mean electrostatic potential in the metal interior. This expression is shown to include all many-body effects and in particular, that of the image force. (This aspect has been reconsidered by Schulte.[126]) Equivalently, the work function may also be computed as the ground-state energy per electron with an additional term to account for the surface dipole.[127] The perturbational method of Lang and Kohn[124] has been generalized by Monnier and Perdew[128] by treating the discrete-lattice effects variationally. This scheme, which ignores the variation of the density in planes parallel to the surface, allows the calculation of the crystal-face dependence of the work function[129] and shows that the effect of the discrete lattice cannot be considered as a weak perturbation. Recently, the pioneering calculation of Bardeen[119] has been reassessed[130] and work functions have been obtained for simple metals using the "displaced-profile change—in—self-consistent-field" approach,[131] still remaining basically in the jellium model.

In the past few years it became apparent that realistic local-density calculations of the electronic structure of simple metal surfaces such as the Al(001) surface[132] and also transition-metal surfaces such as Cu(001) (Ref. 133) and W(001) (Refs. 101 and 134) gave consistently good theoretical results for the work function, usually ± 0.2 eV within the experimental value. The FLAPW method has been demonstrated to be one of the most accurate methods to solve fully self-consistently the local-density equations in the thin-film geometry and we therefore expect from this method work functions close to the local-density limit.

Two main criteria determine the work function (i.e., the

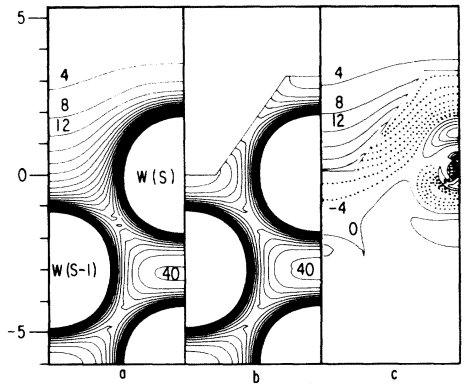

FIG. 14. Total charge density on (a) a clean W(001) surface, (b) an ideal surface, and (c) the difference between (a) and (b), in units of 10^{-3} e/bohr^3. The dotted lines indicate a loss of electronic charge. The vertical scale gives the distance from the surface W atoms in Bohr radii (after Ref. 108).

energy of the Fermi level with respect to the vacuum): the electrostatic surface dipole due to the spill-out of electrons into the vacuum (described by the electrostatic Coulomb potential) and the many-body exchange and correlation effects as incorporated into the effective one-electron potential. Consider first the surface dipole of the clean W(001) surface. One possibility is to monitor the surface dipole by comparing the charge density on the "real" W(001) surface with that of an "ideal" surface, which is constructed by cutting a bulk crystal along the boundaries of nearest-neighbor polyhedra without allowing any charge relaxation. The difference between the charge densities of the real and the ideal surface is due to the spill-out of electrons into the vacuum (Fig. 14). It is remarkable that the charge rearrangement involves essentially only the surface atoms and the influence of the vacuum boundary is mostly screened off already for the subsurface W layer. Associated with the charge-density difference shown in Fig. 14(c) is a surface dipole barrier of 5.5 eV. This is qualitatively in agreement with the result of Smith[121] who finds that the electrostatic double layer is "quite large for the transition metals." It should be noted, however, that the definition of the double layer is not unique. We could have (less realistically) defined an ideal surface by cutting the crystal at a plane halfway between two (001) planes and then compare with the real surface. In that case we would have obtained a much larger "spill-out dipole barrier" of 13.3 eV. The electrostatic Coulomb potential in the (110) plane perpendicular to the surface is shown in Fig. 15 in the form of a three-dimensional (3D) plot for the clean W(001) surface. It is remarkable that we find between the surface atoms regions of positive Coulomb potential. This fact, which indicates a very strong screening, is related to the high, localized electronic density in the surface region. This high density, on the other hand, leads to a large exchange-correlation potential which amounts to -10 eV in the interstitial region inside the metal and leads to the effective one-electron potential shown in Fig. 16 for the clean W(001) surface, which is much deeper than the Coulomb potential. In Fig. 16 we have indicated the Fermi level by the hatched area and the work function Φ as the energy difference between the Fermi level and the vacuum zero. For the five-layer W(001) slab we find a value of 4.77 eV for the work function, which is slightly too high compared to the experimental value of 4.63 ± 0.02 eV.[135] The small discrepancy is presumably due to a thickness effect of the film, since a seven-layer calculation[134] with otherwise the same computational characteristics as our five-layer W(001) calculation gives a work function of 4.63 eV in agreement with experiment.

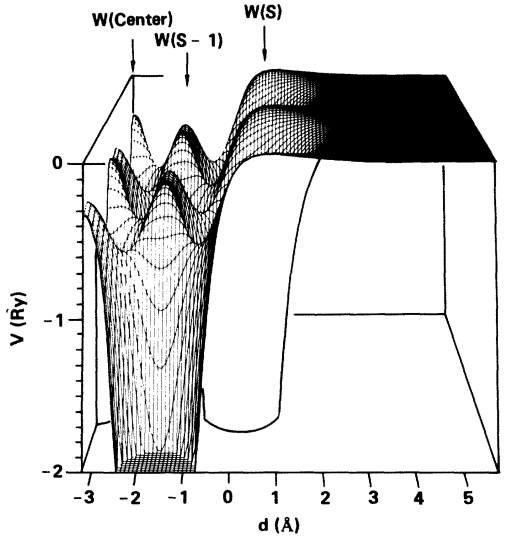

FIG. 15. Electrostatic Coulomb potential in the (110) plane normal to the surface for clean W(001).

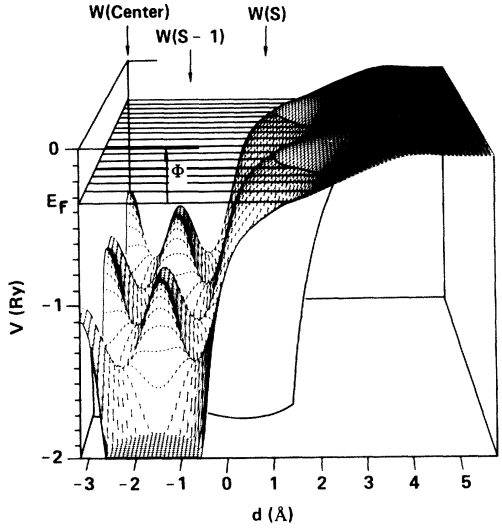

FIG. 16. Effective one-electron potential in the (110) plane normal to the surface for a clean W(001). Φ denotes the work function.

As stated earlier, the charge redistribution at the W(001) surface upon cesiation is localized to the region *outside* the surface W atoms due to the pronounced screening effects. Therefore, the charge density in the interior of the system is not changed and consequently also the exchange-correlation potential remains unaltered. Cs-induced shifts in the Fermi level with respect to the vacuum are therefore completely described by changes in the electrostatic Coulomb potential due to modifications in the surface dipole layer. As discussed in the preceding section, upon cesiation of the W(001) surface, the Cs valence electrons

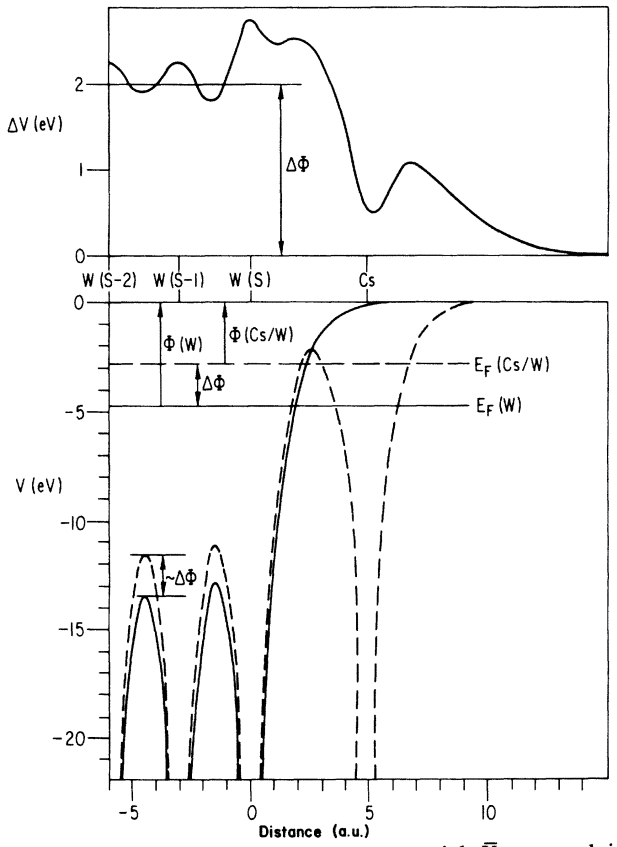

FIG. 17. Lower panel: Coulomb potential $\bar{V}$ averaged in planes parallel to the surface for the clean (solid lines) and the cesiated (dashed lines) W(001) surfaces. Top panel: $\bar{V}$(Cs/W) − [$\bar{V}$(clean W) + $\bar{V}$(Cs monolayer)]. Φ(W) and Φ(Cs/W) denote the work functions of the clean and cesiated W surface, respectively, and ΔΦ is the lowering of the work function. The distance (height) of the Cs atoms to the surface W atoms is 2.60 Å (after Ref. 108).

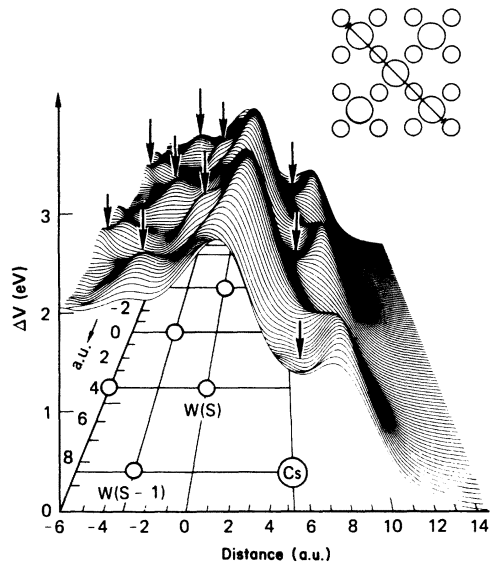

FIG. 18. Electrostatic Coulomb potential barrier originating from the polarizations in a $c(2\times2)$ Cs overlayer ($d = 2.60$ Å) on a W(001) surface (corresponding to the charge redistribution shown in Fig. 13) in the (110) plane perpendicular to the surface as indicated by the inset in the upper right corner.

are polarized towards the W surface leading to an increase of electronic charge in the Cs/W interface region and a depletion of electronic charge outside the Cs overlayer. This gives rise to a dipole barrier whose effect is *opposite* to that of the spill-out dipole: The Cs valence-polarization dipole tends to *decrease* the work function. We also observed in the discussion of the charge density (Fig. 13) a counterpolarization of the Cs 5*p* electrons which leads to an additional, though smaller, dipole barrier which tends to *increase* the work function just as the original spill-out dipole did. Owing to the linearity of Poisson's equation, we obtain the electrostatic potential which corresponds to the overlayer polarizations (i.e., the charge-density difference shown in Fig. 13) simply by taking the difference in the Coulomb potentials of the self-consistent Cs/W case and the superposed potentials of the clean W and the Cs monolayer. The planar average of this difference in Coulomb potentials shown in the top panel of Fig. 17 clearly exhibits the two main Cs-induced dipole barriers: the potential step of 2 eV outside the surface W atoms due to the polarization of the Cs valence electrons and the structure near the Cs atoms originating from the counterpolarizations of the Cs 5*p* electrons. The net result of the Cs-induced dipoles is a raising[136] of the mean electrostatic potential in the interior of the cesiated metal surface, a corresponding rise of the Fermi energy with respect to the vacuum and, therefore, a lowering of the work function. The detailed structure of the Cs-induced potential barriers, represented in the form of a 3D plot in Fig. 18, demonstrates this situation very impressively. We recognize in Fig. 18 the 2-eV barrier originating from the polarization of the Cs valence electrons and the balconylike structures due to the counterpolarization of the Cs 5*p* electrons. The plateau on the left-hand side of Fig. 19 represents the essentially constant shift of the potential in the interior of the system. The Coulomb potential of the cesiated W(001) surface, shown in Fig. 19, resembles inside the W surface (left-hand side of Fig. 19) that of the clean W(001) surface (Fig. 15) except for the fact that it is shifted by 2 eV to higher energies. Since, as stated earlier, the exchange-

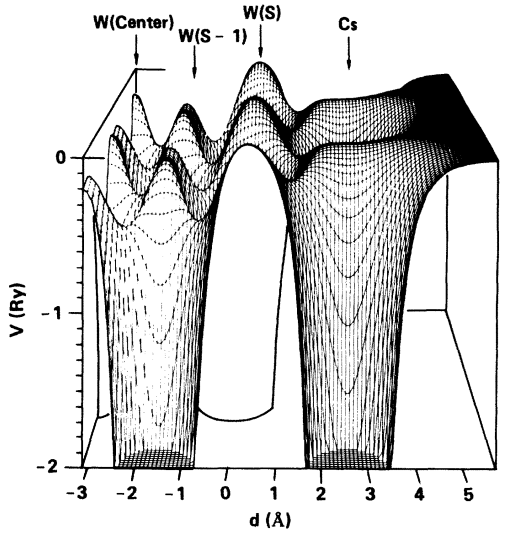

FIG. 19. Coulomb potential for $c(2\times2)$ Cs on W(001) ($d = 2.60$ Å) in the (110) plane perpendicular to the surface.

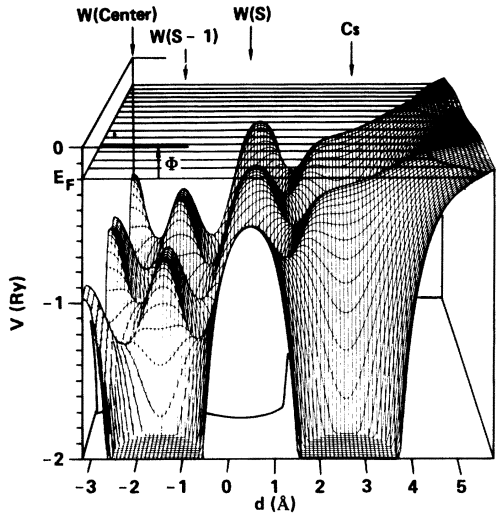

FIG. 20. Effective one-electron potential for $c(2\times2)$ Cs on W(001) ($d=2.60$ Å) in the (110) plane perpendicular to the surface. Φ denotes the work function of this system.

correlation contribution to the potential inside the surface remains unaltered upon cesiation, the effective potential (Fig. 20) is shifted by the same amount (2 eV) as the Coulomb potential. As a consequence, the Fermi energy is also shifted by 2 eV to higher energies with respect to the vacuum (compare Figs. 15 and 20) and thus the work function is lowered. As the distance of the Cs atoms from the W surface is increased from 2.60 to 2.90 Å, the work function of the cesiated surfaces is changed markedly from 2.77 to 2.28 eV. The main reason seems to be that upon separation the thickness of the polarized Cs overlayer is extended and consequently its dipole moment increased, and this leads to a further lowering of the work function. It is important to note that the multiple dipoles which reduce the work function are essentially located *outside* the surface W atoms. Therefore, the simple classical dipole picture of a Cs^+ ion and its image charge *inside* the metal surface is inadequate.

The values of the work functions are found to be 4.77 eV for the clean five-layer W(001) film, and 2.77, 2.55, and 2.28 eV for $c(2\times2)$ Cs on the five-layer W slab with d(Cs-W)=2.60, 2.75, and 2.90 Å, respectively. For the Cs monolayer we find a work function of 2.37 eV.

The experimental value of the work function for the monolayer coverage ($\Theta\approx0.50$) is given by 1.8 eV.[21] From our calculation we would, therefore, extrapolate the height of the Cs atoms to be 3.1 Å. Assuming a bridge position as an adsorption site in the monolayer coverage[19] we would then get a Cs—W bond distance of 3.48 Å. If we make the additional assumption that the Cs—W bond length remains the same for Cs positioned in a fourfold hollow site as in the $p(2\times2)$ structure and in our calculations, we would get for this hollow-site adsorption geometry a Cs height of 2.7 Å. However, there is a possibility that we overestimated the Cs 5p counterpolarization due to the semirelativistic rather than the fully relativistic treatment of the valence electrons, including the Cs 5p "semicore." Thus our calculated work functions for the cesiated surface could be slightly too large. Clearly, further experimental and theoretical effort is needed to establish the height of the Cs atoms on a W(001) surface.

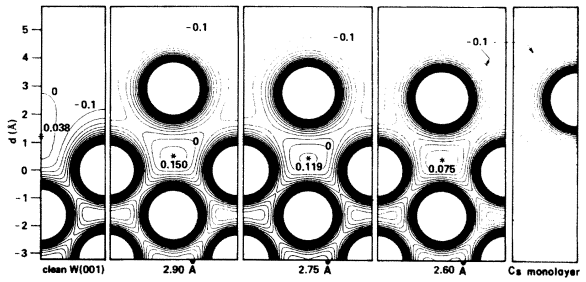

FIG. 21. Coulomb potential for a clean W(001) five-layer slab (left panel) and $c(2\times2)$ Cs on the W(001) slab for Cs heights of 2.60, 2.75, and 2.90 Å (central panels) in the (110) plane perpendicular to the surface. The Coulomb potential for the Cs monolayer is shown in the right panel.

Closely related to the Cs-induced changes in the electrostatic Coulomb potential and in the effective one-electron potential is the question of core-level shifts which provide an interesting experimental tool in probing the local potentials. We, therefore, reconsider the Coulomb potentials (Fig. 21) and the effective potentials (Fig. 22) of all systems studied in the present work. From Figs. 21 and 22 and from the discussion of the Cs-induced changes in the surface potential barrier it is obvious that for the cesiated surface all W core levels are shifted to smaller binding energies with respect to the vacuum. (However, their relative position with respect to the Fermi level remains essentially unchanged.) The Coulomb potential near the Cs atom is found to be less attractive in all three cases of Cs on W(001) shown in Fig. 21 than in the unsupported Cs monolayer given to the right of Fig. 21. The same situation is found for the effective potentials shown in Fig. 22. As a consequence, all Cs core eigenvalues are expected to be shifted to smaller binding energies with respect to the vacuum as Cs is adsorbed on the W(001) surface. As a matter of fact, the Cs 3s level, for example, which is found at -85.539 Ry for the free Cs atom and at -85.929 Ry for the free Cs^+ ion, is shifted up to -85.440 Ry for Cs on W(001) with a height of the Cs atoms of 2.60 Å. Similar trends are found also for the other Cs core levels. A compilation of selected core-level shifts is given in Table I. It is interesting to note how little (less than 0.4 eV) the core levels in the clean W five-layer slab deviate from

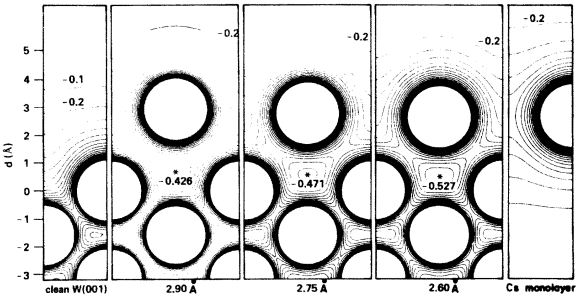

FIG. 22. Effective one-electron potential for a clean W(001) five-layer slab (left panel) and $c(2\times2)$ Cs on the W(001) slab for Cs heights of 2.60, 2.75, and 2.90 Å (central panels) in the (110) plane perpendicular to the surface. The effective potential for the Cs monolayer is shown in the right panel.

TABLE I. Shift of local-density one-particle energies with respect to the corresponding core levels of free atoms in eV, i.e., ϵ_i(surface) $-\epsilon_i$(atom).

		$c(2\times2)$ Cs on W(001)		
	Clean W(001)	$d=2.60$ Å	$d=2.75$ Å	$d=2.90$ Å
Cs				
5s		1.40	1.57	1.70
4s		1.36	1.52	1.65
3s		1.35	1.50	1.62
2s		1.33	1.48	1.61
1s		1.24	1.40	1.52
W(S)				
$4f_{5/2}$	−0.19	2.19	2.41	2.59
5s	−0.08	2.25	2.48	2.68
4s	−0.22	2.16	2.39	2.56
3s	−0.26	2.14	2.37	2.52
2s	−0.34	2.10	2.31	2.45
1s	−0.34	2.16	2.33	2.46
W($S-1$)				
$4f_{5/2}$	−0.01	2.20	2.49	2.72
5s	−0.05	2.20	2.49	2.72
4s	−0.00	2.20	2.44	2.71
3s	−0.03	2.19	2.41	2.69
2s	−0.08	2.15	2.38	2.65
1s	−0.03	2.25	2.44	2.72
W(center)				
$4f_{5/2}$	−0.22	1.95	2.22	2.46
5s	−0.19	1.96	2.22	2.46
4s	−0.25	1.93	2.22	2.46
3s	−0.27	1.92	2.20	2.44
2s	−0.33	1.88	2.16	2.41
1s	−0.26	1.95	2.23	2.48

those of a free W atom. We find for this W slab an oscillation for the layers S, $S-1$, and center, which does not allow us to make a clear statement about core-level shifts on a clean W(001) surface. However, a seven-layer slab calculation[134] indicates a core-level shift to smaller binding energies at the clean W(001) surface. Upon cesiation, all W core levels are shifted to smaller binding energies—as expected from the changes in the Coulomb potential. All Cs core levels are shifted to smaller binding energies compared to the free, neutral Cs atom.

VI. SUMMARY AND CONCLUSIONS

We have studied the electronic structure of a $c(2\times2)$ Cs overlayer on a W(001) surface by means of highly accurate, fully self-consistent, all-electron calculations using our FLAPW method for thin films within local-density–functional theory. The clean W(001) surface was represented by a single slab of five layers of W. Cs was deposited in the form of $c(2\times2)$ overlayers on both sides of the five-layer W slab resulting in a unit cell with 12 atoms. Independent self-consistent calculations were performed for three distances between the planes of the Cs and surface W atoms, namely $d=2.60$, 2.75, and 2.90 Å. For comparison, a self-consistent calculation for the Cs monolayer with the same Cs-Cs distance as in the $c(2\times2)$ overlayer on W(001) was also carried out.

We found that upon cesiation the occupied part of the energy-band structure of W is not changed drastically. The characteristic high density of W surface states and surface resonance states near the Fermi energy persists for the cesiated W surface. The interaction between the Cs valence states (originating from the atomic Cs 6s levels) and the W d surface states leads to a hybridization of these states and causes these predominantly W d-like states to be stabilized energetically. The most striking effect is seen for the d_{z^2}-like W surface state at $\bar{\Gamma}_1$ just below the Fermi energy: This state is lowered in energy by 1 eV upon cesiation.[137] The Cs 5p semicore states are found to interact markedly with the W s-like states, particularly those at the bottom of the W s band.

The valence charge density in the surface region is mostly dominated by the W states. The spillout of W electrons into the vacuum leads for the cesiated surface to an increase in valence charge near the Cs nuclei compared with the isolated Cs monolayer. Upon cesiation the Cs valence electrons are found to be polarized towards the W surface resulting in a depletion of electronic charge between and outside the Cs nuclei and an increase of electronic charge in the Cs/W interface region. The Cs 5p semicore electrons show a polarization opposite to that of the Cs valence electrons. These multiple polarizations within the Cs overlayer amount to a net reduction of the spill-out dipole and hence bring about the lowering of the work function upon cesiation. The Cs-induced changes in the charge density and in the surface dipole are essentially confined to the region *outside* the surface W atoms. Thus the simple classical picture of Cs donating an electron *into* the metal, becoming a Cs^+ ion, and forming a dipole with its negative-image charge is inadequate. Presumably, also for lower coverages the charge redistribution will take place essentially *outside* the W surface atoms. However, the fact that the minimum of the work function for the Cs/W(001) system occurs at half Cs coverage studied in the present work shows that at lower coverages the polarization of the Cs atoms becomes more pronounced.

In conclusion, we find that Cs on a W(001) surface at a coverage of one Cs atom for two W atoms forms a polarized-metallic rather than ionic overlayer. Important for a realistic picture of the surface is the fact that the valence charge density in the surface region is strongly dominated by the W d-like states. It is the interaction of the surface W atoms with their d-like states and the Cs valence electrons originating from the atomic 6s states, which results in the polarization of the Cs valence electrons. Surprisingly, the Cs 5p semicore electrons participate greatly in the bond formation due to their interactions with the electrons at the bottom of the W s band. The net redistribution of the Cs 5p states upon cesiation can be described as a counterpolarization to the polarization induced by the Cs valence electrons.

It is crucial that most of the surface states and surface resonance states of the W(001) surface persist even after cesiation and retain the high density of surface states and surface resonance states so characteristic of the W(001) surface. This means that the electronic structure of the W substrate remains important even if the surface is covered with a Cs overlayer. It will be extremely interesting and

relevant to investigate if the W(001) surface is a special case or if this importance of the substrate is a general feature of cesiated transition-metal surfaces. Experimental and theoretical effort is needed to settle the question of the height of the Cs atoms, which was shown to be important for quantitative statements about the work function.

ACKNOWLEDGMENTS

We are grateful to H. Krakauer and M. Weinert for close cooperation during the early phases of this work and to S. Ohnishi for making available his W seven-layer results and for helpful discussions. We would also like to thank Dr. R. Riwan for sending us copies of the unpublished experimental work by Soukiassian *et al.*,[137] which confirms the 1-eV shift of the $\bar{\Gamma}_1$ SS. It is a pleasure for us to acknowledge the excellent cooperation and the competent service of the Magnetic Fusion Energy Computing Center. This work was supported by the National Science Foundation, Materials Research Laboratory program, through the Materials Research Center of Northwestern University (Grant No. DMR-79-23573), the U.S. Navy Office of Naval Research (Grant No. N00014-81-K-0438), and the U.S. Department of Energy (Contract No. W-7405-ENG-48).

*Permanent address: Institut für Physikalische Chemie, Universität Wien, Währingerstrasse 42, A-1090 Vienna, Austria.

[1]K. H. Kingdon and I. Langmuir, Phys. Rev. 21, 380 (1923).
[2]J. A. Becker, Phys. Rev. 28, 341 (1926).
[3]A. H. Sommer, *Photoemissive Materials* (Wiley, New York, 1968).
[4]G. N. Hatsopoulos and E. P. Gyftopoulos, *Thermionic Energy Conversion* (MIT, Cambridge, Mass., 1979).
[5]S. G. Forbes, in *Jet, Rocket, Nuclear and Electric Propulsion: Theory and Design,* Vol. 7 of *Applied Physics and Engineering* (Springer, New York, 1968), p. 442.
[6]Y. I. Belchenko, G. I. Dimov, and V. G. Dudnikov, Nucl. Fusion 14, 113 (1974); K. Prelec and Th. Sluyters, Second Symposium on Ion Sources and Formation of Ion Beams, Berkeley, California, 1974 (unpublished); Lawrence Berkeley Laboratory Report No. LBL-3399 (unpublished).
[7]K. N. Leung and K. W. Ehlers, Rev. Sci. Instrum. 53, 803 (1982); P. J. Schneider, K. H. Berkner, W. G. Graham, R. V. Pyle, and J. W. Stearns, Phys. Rev. B 23, 941 (1981); A. Pargellis and M. Seidl, *ibid.* 25, 4356 (1982); M. Seidl and A. Pargellis, *ibid.* 26, 1 (1982); J. N. M. van Wunnik, B. Rasser, and J. Los, Phys. Lett. 87A, 288 (1982); B. Rasser, J. N. M. van Wunnik, and J. Los, Surf. Sci. 118, 697 (1982); P. J. Schneider, W. Eckstein, and H. Verbeck, Nucl. Instrum. Methods 194, 387 (1982).
[8]J. R. Hiskes, A. Karo, and M. Gardner, J. Appl. Phys. 47, 3888 (1976); J. R. Hiskes, J. Phys. (Paris) Colloq. 40, C7-179 (1979); J. R. Hiskes and P. J. Schneider, in *Low-Energy Ion Beams, Bath, 1980,* edited by I. H. Wilson and K. G. Stephens (IOP, London, 1980), Vol. 54, Chap. 5, p. 182; J. Nucl. Mater. 93-94, 536 (1980); Phys. Rev. B 23, 949 (1981).
[9]I. Langmuir and J. B. Taylor, Phys. Rev. 40, 463 (1932).
[10]J. B. Taylor and I. Langmuir, Phys. Rev. 44, 423 (1933).
[11]H. Utsugi and R. Gomer, J. Chem. Phys. 37, 1720 (1962).
[12]L. W. Swanson and R. W. Strayer, J. Chem. Phys. 48, 2421 (1968).
[13]H. Utsugi and R. Gomer, J. Chem. Phys. 37, 1706 (1962).
[14]L. Schmidt and R. Gomer, J. Chem. Phys. 42, 3573 (1965).
[15]A. U. MacRae, K. Müller, J. J. Lander, J. Morrison, and J. C. Phillips, Phys. Rev. Lett. 22, 1048 (1969).
[16]A. U. MacRae, K. Müller, J. J. Lander, and J. Morrison, Surf. Sci. 15, 483 (1969).
[17]D. L. Fehrs, T. J. Lee, B. J. Hopkins, and R. E. Stickney, Surf. Sci. 21, 197 (1970).
[18]T. J. Lee, B. H. Blott, and B. J. Hopkins, J. Phys. F 1, 309 (1971).
[19]V. B. Voronin, A. G. Naumovets, and A. G. Fedorus, Zh. Eksp. Teor. Fiz. Pis'ma Red 15, 523 (1972) [JETP Lett. 15, 370 (1972)].
[20]C. A. Papageorgopoulos and J. M. Chen, Surf. Sci. 39, 283 (1973).
[21]J. L. Desplat, Surf. Sci. 34, 588 (1973).
[22]C. A. Papageorgopoulos and J. M. Chen, Surf. Sci. 39, 313 (1973).
[23]J. L. Desplat, Jpn. J. Appl. Phys. Suppl. 2, 177 (1974).
[24]C. A. Papageorgopoulos and J. M. Chen, J. Vac. Sci. Technol. 9, 570 (1972).
[25]J.-L. Desplat and C. A. Papageorgopoulos, Surf. Sci. 92, 97 (1980).
[26]C. A. Papageorgopoulos and J.-L. Desplat, Surf. Sci. 92, 119 (1980).
[27]Chen-Show Wang, J. Appl. Phys. 48, 1477 (1977).
[28]C. J. Todd and T. N. Rhodin, Surf. Sci. 42, 109 (1974).
[29]E. V. Klimenko and A. G. Naumovets, Surf. Sci. 14, 141 (1969).
[30]P. Akhter and J. A. Venables, Surf. Sci. 102, L41 (1981).
[31]P. Akhter and J. A. Venables, Surf. Sci. 103, 301 (1981).
[32]I. Langmuir and K. H. Kingdon, Phys. Rev. 21, 381 (1923).
[33]I. Langmuir, J. Am. Chem. Soc. 54, 2798 (1932).
[34]I. Langmuir, Phys. Rev. 43, 224 (1933).
[35]R. W. Gurney, Phys. Rev. 47, 479 (1935).
[36]I. Higuchi, T. Ree, and H. Eyring, J. Am. Chem. Soc. 77, 4969 (1955).
[37]I. Higuchi, T. Ree, and H. Eyring, J. Am. Chem. Soc. 79, 1330 (1957).
[38]J. H. De Boer, in *Advances in Catalysis,* edited by W. G. Frankenburg, V. I. Komarewsky, and. E. K. Rideal (Academic, New York, 1956), Vol. 8, p. 17.
[39]N. S. Rasor and C. Warner, J. Appl. Phys. 35, 2589 (1964).
[40]C. Warner, *Thermionic Conversion Specialists Conference, San Diego, 1971* (IEEE, New York, 1972), p. 170.
[41]J. W. Gadzuk and E. N. Carabateas, J. Appl. Phys. 36, 357 (1965).
[42]J. R. MacDonald and C. D. Barlow, Jr., J. Chem. Phys. 40, 1535 (1964); 43, 2575 (1965); 44, 202 (1966).
[43]J. Becker, *Advances in Catalysis,* edited by W. G. Frankenburg, V. I. Komarewsky, and E. K. Rideal (Academic, New York, 1955), Vol. 7, p. 135.
[44]B. M. W. Trapnell, *Chemisorption* (Butterworths, London, 1957), p. 147.
[45]F. L. Hughes, Phys. Rev. 113, 1036 (1959).
[46]F. L. Hughes and H. Levinstein, Phys. Rev. 113, 1029 (1959).
[47]G. E. Moore and H. W. Allison, J. Chem. Phys. 23, 1609 (1955).
[48]D. D. Eley, Discuss. Faraday Soc. 8, 34 (1950).

[49]D. P. Stevenson, J. Chem. Phys. 23, 203 (1955).
[50]T. B. Grimley, in *Advances in Catalysis,* edited by D. D. Eley, P. W. Selwood, and P. B. Weisz (Academic, New York, 1960), Vol. 12, p. 1.
[51]W. E. Danforth, J. Appl. Phys. 33, 1972 (1962).
[52]E. Ya. Zandberg, Zh. Tekh. Fiz. 30, 206 (1960) [Sov. Phys.—Tech. Phys. 5, 186 (1961)].
[53]V. M. Gavriluk, Ukr. Fiz. Zh. 4, 734 (1959).
[54]J. D. Levine and E. P. Gyftopoulos, Surf. Sci. 1, 171 (1964).
[55]H. E. Albrecht, Phys. Status Solidi A 6, 135 (1971).
[56]H. E. Albrecht, Phys. Status Solidi A 9, 125 (1972).
[57]T. B. Grimley, J. Phys. Chem. Solids 14, 227 (1960).
[58]A. J. Bennett and L. M. Falicov, Phys. Rev. 151, 512 (1966).
[59]A. J. Bennett, J. Chem. Phys. 49, 1340 (1968).
[60]J. W. Gadzuk, Surf. Sci. 6, 133 (1967).
[61]J. W. Gadzuk, J. K. Hartmann, and T. N. Rhodin, Phys. Rev. B 4, 241 (1971).
[62]O. M. Braun, L. C. Il'chenko, E. A. Pashitskii, Fiz. Tverd. Tela. (Leningrad) 22, 1649 (1980) [Sov. Phys.—Solid State 22, 963 (1980)].
[63]D. M. Newns, J. Chem. Phys. 50, 4572 (1969).
[64]D. M. Newns, Phys. Rev. 178, 1123 (1969); B 1, 3304 (1970).
[65]J. P. Muscat and D. M. Newns, Solid State Commun. 11, 737 (1972).
[66]J. P. Muscat and D. M. Newns, J. Phys. C 7, 2630 (1974).
[67]J. P. Muscat and D. M. Newns, Surf. Sci. 84, 262 (1979).
[68]S. C. Ying, J. R. Smith, and W. Kohn, Phys. Rev. B 11, 1483 (1975).
[69]N. D. Lang and A. R. Williams, Phys. Rev. Lett. 34, 531 (1975).
[70]N. D. Lang and A. R. Williams, Phys. Rev. B 16, 2408 (1977).
[71]S. M. Dunaerskii, Fiz. Tverd. Tela. (Leningrad) 19, 3062 (1977) [Sov. Phys.—Solid State 19, 1790 (1977)].
[72]N. D. Lang and A. R. Williams, Phys. Rev. B 18, 616 (1978).
[73]N. D. Lang, Phys. Rev. Lett. 46, 842 (1981).
[74]N. D. Lang, Phys. Rev. B 4, 4234 (1971).
[75]N. D. Lang, Solid State Commun. 9, 1015 (1971).
[76]H. Yamauchi and U. Kawabe, Phys. Rev. B 14, 2687 (1976).
[77]P. W. Anderson, Phys. Rev. 124, 41 (1961).
[78]U. Fano, Phys. Rev. 124, 1866 (1961).
[79]P. Hohenberg and W. Kohn, Phys. Rev. 136, B864 (1964).
[80]W. Kohn and L. J. Sham, Phys. Rev. 140, A1133 (1965).
[81]K. F. Wojciechowski, Acta Phys. Polon. 29, 119 (1966).
[82]K. F. Wojciechowski, Acta Phys. Polon. 33, 363 (1968).
[83]T. B. Grimley, in *Electronic Structure and Reactivity of Metal Surfaces,* edited by E. G. Derouane and A. A. Lucas (Plenum, New York, 1976), p. 35.
[84]J. R. Schrieffer, in *Dynamic Aspects of Surface Physics,* edited by F. O. Goodman (Editrice Compositori, Bologna, 1974), p. 250.
[85]R. Gomer, in *Solid State Physics,* edited by F. Seitz, D. Turnbull, and H. Ehrenreich (Academic, New York, 1975), Vol. 30, p. 93.
[86]J. W. Gadzuk, in *Surface Physics of Materials,* edited by J. M. Blakely (Academic, New York, 1975), Vol. II, p. 339.
[87]B. I. Lundqvist, H. Hjelmberg, and O. Gunnarsson, in *Photoemission and the Electronic Properties of Surfaces,* edited by B. Feuerbacher, B. Fitton, and R. F. Willis (Wiley, New York, 1978), p. 227.
[88]F. J. Arlinghaus, J. G. Gay, and J. R. Smith, in *Theory of Chemisorption,* edited by J. R. Smith (Springer, Berlin, 1980), p. 71.
[89]V. L. Moruzzi, J. F. Janak, and A. R. Williams, *Calculated Electronic Properties of Metals* (Pergamon, New York, 1978).
[90]D. D. Koelling, Rep. Prog. Phys. 44, 139 (1981).
[91]J. Harris and R. O. Jones, J. Chem. Phys. 70, 830 (1979).
[92]J. A. Appelbaum and D. R. Hamann, Phys. Rev. B 6, 2166 (1972).
[93]C. S. Wang and A. J. Freeman, Phys. Rev. B 19, 793 (1979); 19, 4930 (1979).
[94]J. R. Smith, J. G. Gay, and F. J. Arlinghaus, Phys. Rev. B 21, 2201 (1980); see also Ref. 88.
[95]D. R. Hamann, L. F. Mattheis, and H. S. Greenside, Phys. Rev. B 24, 6151 (1981).
[96]P. M. Marcus, Int. J. Quantum Chem. 1, 567 (1967).
[97]O. K. Andersen, Phys. Rev. B 12, 3060 (1975).
[98]D. D. Koelling and G. O. Arbman, J. Phys. F 5, 2041 (1975).
[99]O. Jepsen, J. Madsen, and O. K. Andersen, Phys. Rev. B 18, 605 (1978).
[100]H. Krakauer, M. Posternak, and A. J. Freeman, Phys. Rev. B 19, 1706 (1979).
[101]M. Posternak, H. Krakauer, A. J. Freeman, and D. D. Koelling, Phys. Rev. B 21, 5601 (1980).
[102]H. Krakauer, M. Posternak, and A. J. Freeman, Phys. Rev. Lett. 43, 1885 (1979).
[103]Ding-Sheng Wang, A. J. Freeman, H. Krakauer, and M. Posternak, Phys. Rev. B 23, 1685 (1981).
[104]Ding-Sheng Wang, A. J. Freeman, and H. Krakauer, Phys. Rev. B 24, 1126 (1981); 24, 3092 (1981); 24, 3104 (1981).
[105]G. A. Benesh, H. Krakauer, D. E. Ellis, and M. Posternak, Surf. Sci. 104, 599 (1981).
[106]D. S. Wang, A. J. Freeman, and H. Krakauer, Phys. Rev. B 26, 1340 (1982).
[107]E. Wimmer, H. Krakauer, M. Weinert, and A. J. Freeman, Phys. Rev. B 24, 864 (1981).
[108]E. Wimmer, A. J. Freeman, M. Weinert, H. Krakauer, J. R. Hiskes, and A. M. Karo, Phys. Rev. Lett. 48, 1128 (1982).
[109]D. Pines, *Elementary Excitations in Solids* (Benjamin, New York, 1963). Equation (3.58) gives the expression for $E_{\rm corr}$, where $V_{\rm corr}=\delta\rho E_{\rm corr}/\delta\rho$, and $V_{xc}=V_{\rm corr}-1.969\,490\,044\rho^{1/3}$.
[110]M. Weinert, E. Wimmer, and A. J. Freeman, Phys. Rev. B 26, 4571 (1982).
[111]B. Delley, A. J. Freeman, M. Weinert, and E. Wimmer, Phys. Rev. B 27, 6509 (1983).
[112]M. Weinert, J. Math. Phys. (N.Y.) 22, 2433 (1981).
[113]D. G. Anderson, J. Assoc. Comp. Mach. 12, 547 (1965).
[114]D. R. Hamann (private communication).
[115]Shang-Lin Weng, E. W. Plummer, and T. Gustafsson, Phys. Rev. B 18, 1718 (1978), and references therein.
[116]M. I. Holmes and T. Gustafsson, Phys. Rev. Lett. 47, 443 (1981).
[117]J. C. Campuzano, J. E. Inglesfield, D. A. King, and C. Somerton, J. Phys. C 14, 3099 (1981).
[118]E. Wigner and J. Bardeen, Phys. Rev. 48, 84 (1935).
[119]J. Bardeen, Phys. Rev. 49, 653 (1936).
[120]A. J. Bennett and C. B. Duke, in *Structure and Chemistry of Solid Surfaces,* edited by G. A. Somorjai (Wiley, New York, 1969).
[121]J. R. Smith, Phys. Rev. 181, 522 (1969).
[122]N. D. Lang, Solid State Commun. 7, 1047 (1969).
[123]N. D. Lang and W. Kohn, Phys. Rev. B 1, 4555 (1970).
[124]N. D. Lang and W. Kohn, Phys. Rev. B 3, 1215 (1971).
[125]R. Smoluchowski, Phys. Rev. 60, 661 (1941).
[126]F. K. Schulte, Z. Phys. B 27, 303 (1977).
[127]G. D. Mahan and W. L. Schaich, Phys. Rev. B 10, 2647 (1974).
[128]R. Monnier and J. P. Perdew, Phys. Rev. B 17, 2595 (1978).
[129]R. Monnier, J. P. Perdew, D. C. Langreth, and J. W. Wilkins,

Phys. Rev. B 18, 656 (1978).
[130]V. Sahni and C. Q. Ma, Phys. Rev. B 22, 5987 (1980).
[131]V. Sahni, J. P. Perdew, and J. Gruenebaum, Phys. Rev. B 23, 6512 (1981).
[132]E. Wimmer, M. Weinert, A. J. Freeman, and H. Krakauer, Phys. Rev. B 24, 2292 (1981).
[133]J. G. Gay, J. R. Smith, and F. K. Arlinghaus, Phys. Rev. Lett. 42, 332 (1979); J. R. Smith, J. G. Gay, and F. J. Arlinghaus, Phys. Rev. B 21, 2201 (1980).
[134]S. Ohnishi, E. Wimmer, and A. J. Freeman, Bull. Am. Phys. Soc. 27, 210 (1982) and unpublished.
[135]R. L. Billington and T. N. Rhodin, Phys. Rev. Lett. 41, 1602 (1978).
[136]We adopt here the convention and define the zero of the potential scale as the vacuum potential at infinite distance from the surface. Equivalently, one could define the zero as the average Coulomb potential of the bulk W unit cell. The potential and the Fermi energy inside the film would then remain constant upon cesiation. The first more natural convention has the advantage of being numerically better defined.
[137]Very recent measurements by P. Soukiassian, R. Riwan, C. Guillot, J. Lecante, and Y. Borensztein (private communication) confirm our prediction of the 1-eV shift of the $\bar{\Gamma}_1$ SS upon cesiation.

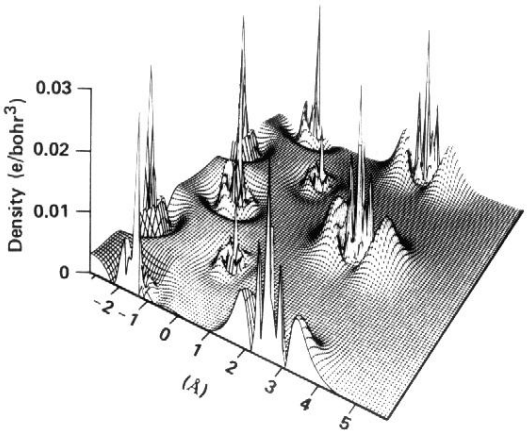

FIG. 10. Single-particle density of the $\bar{\Gamma}_1$ state at the bottom of the W valence band for $c(2\times2)$ Cs on W(001) with d(Cs-W)=2.60 Å. The density units are e/bohr^3.

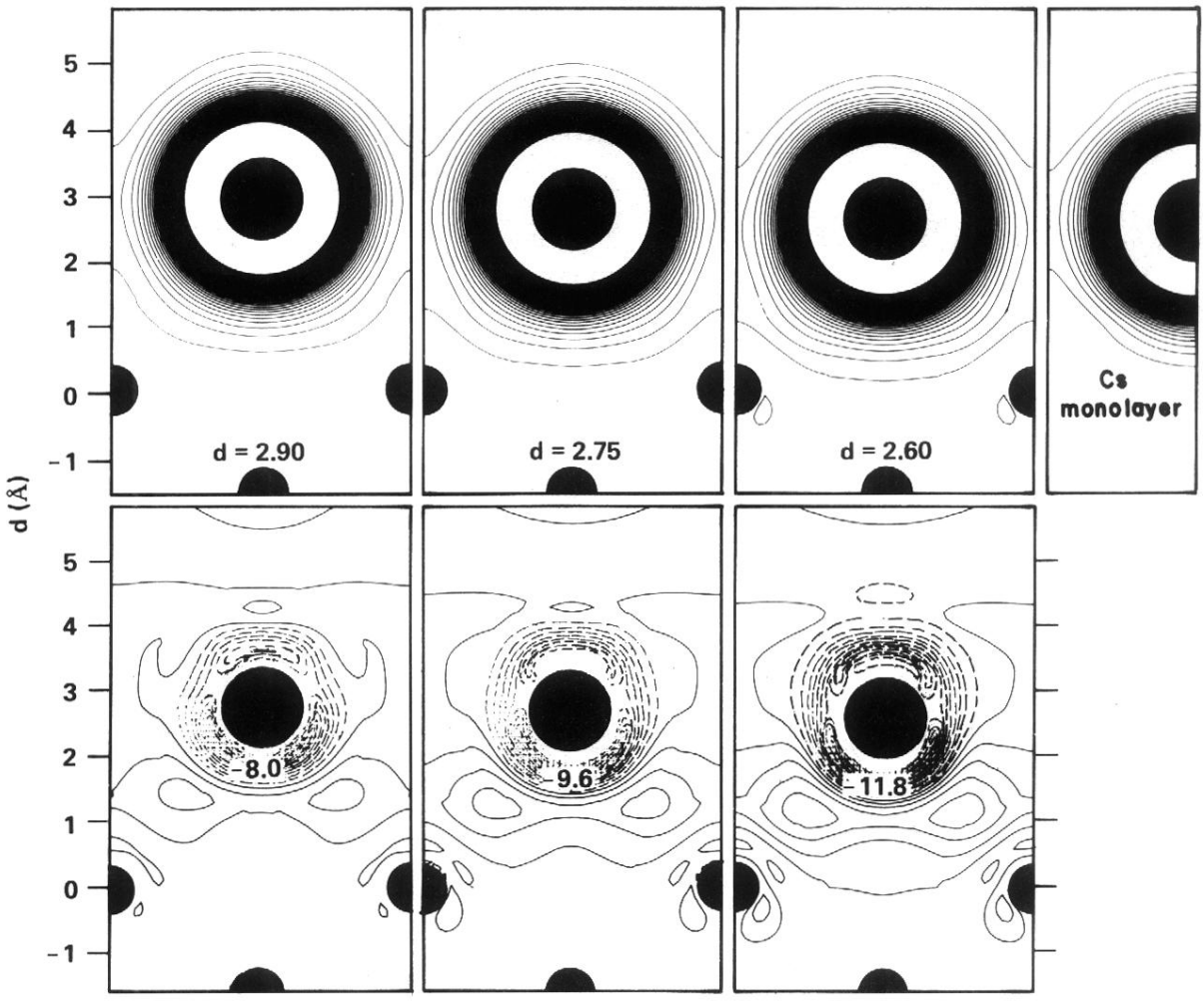

FIG. 11. Upper panels: charge density originating from the Cs $5p$ band. The lowest contour and the contour spacing are 1×10^{-3} e/bohr^3. Lower panels: the difference ρ_{5p}(Cs/W)$-\rho_{5p}$(Cs monolayer) with a contour spacing of 0.5×10^{-3} e/bohr^3.

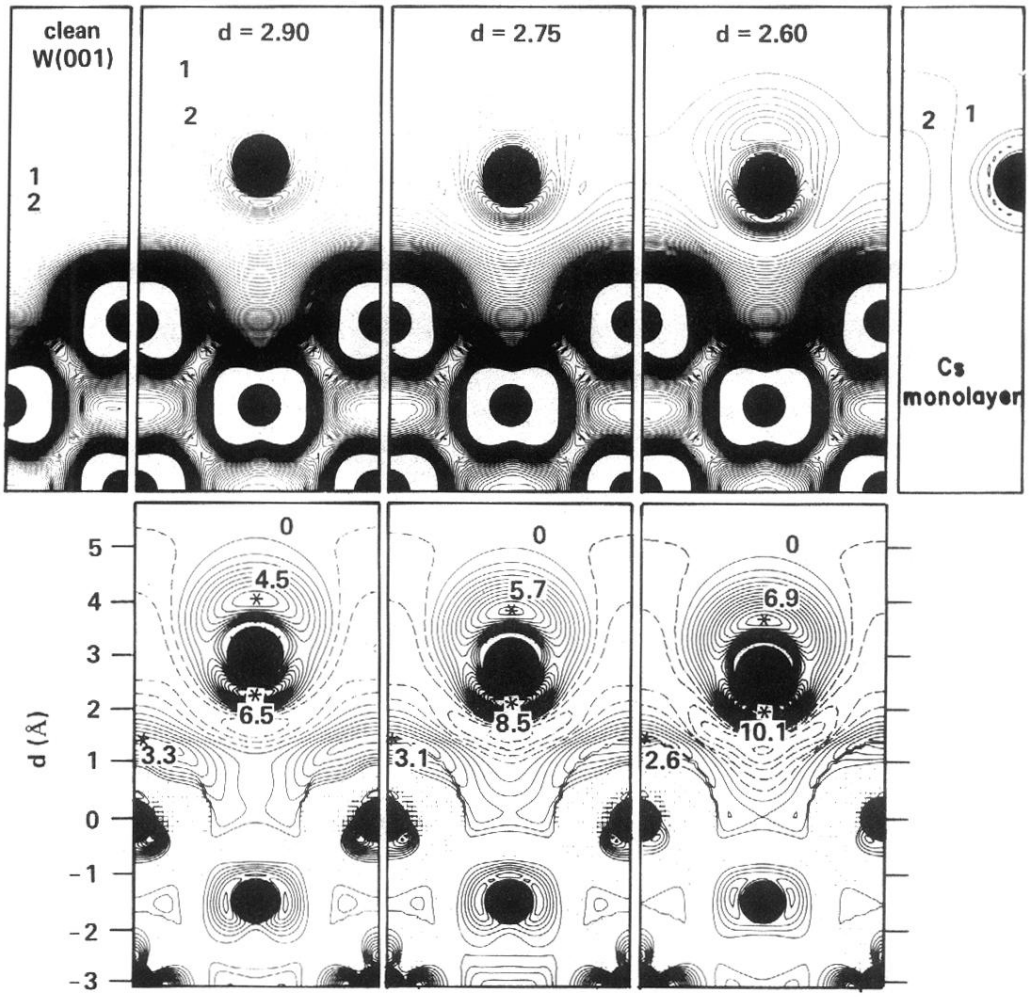

FIG. 12. Upper panels: charge density originating from the W valence band. The lowest contour and the contour spacings are 1×10^{-3} e/bohr^3. The contour plot is cutoff at a density of 75×10^{-3} e/bohr^3. Lower panels: the difference $\rho_{\text{val}}(\text{Cs-W})-\rho_{\text{val}}(\text{W})$ with a contour spacing of 0.5×10^{-3} e/bohr^3.

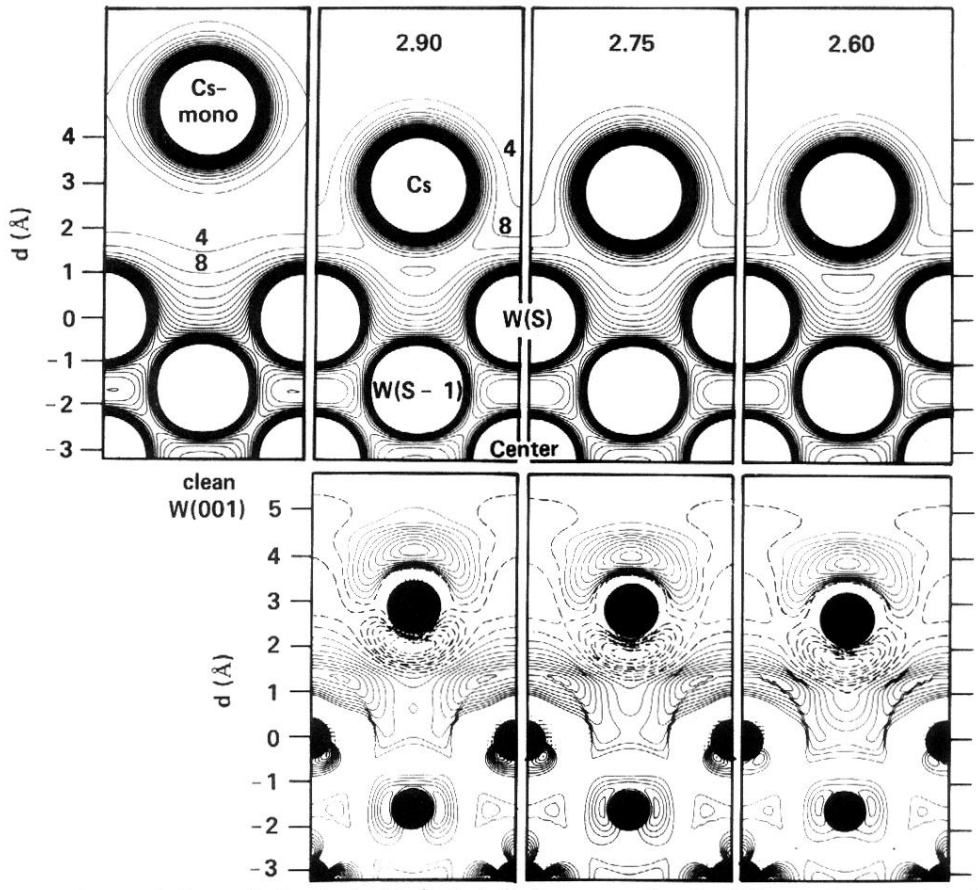

FIG. 13. Upper panels: total electronic density in 10^{-3} e/bohr^3. Lower panels: the difference between the self-consistent density of the cesiated surfaces and the superposed density of a clean W five-layer film and a Cs monolayer.

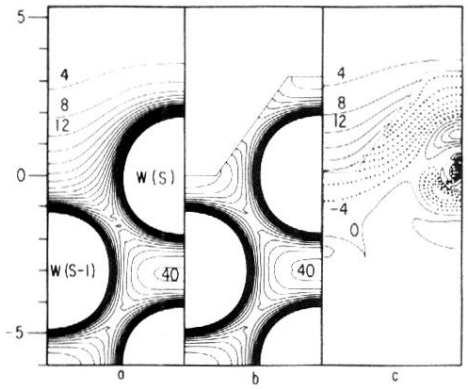

FIG. 14. Total charge density on (a) a clean W(001) surface, (b) an ideal surface, and (c) the difference between (a) and (b), in units of 10^{-3} e/bohr^3. The dotted lines indicate a loss of electronic charge. The vertical scale gives the distance from the surface W atoms in Bohr radii (after Ref. 108).

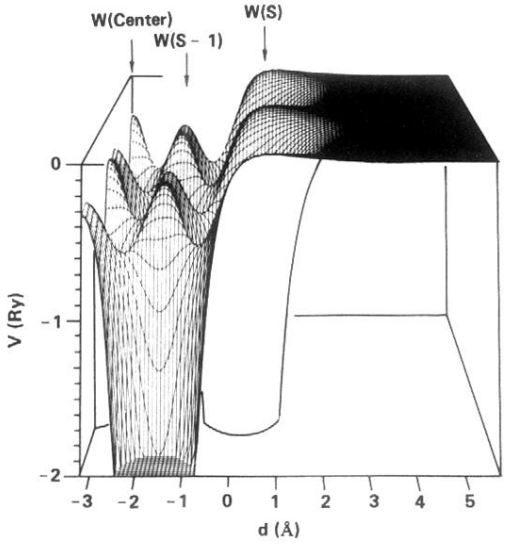

FIG. 15. Electrostatic Coulomb potential in the (110) plane normal to the surface for clean W(001).

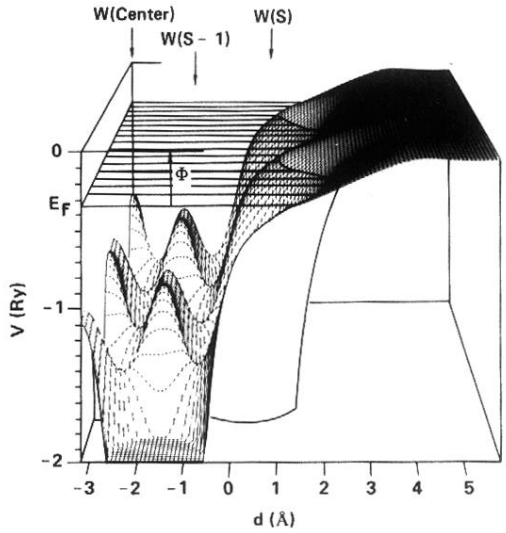

FIG. 16. Effective one-electron potential in the (110) plane normal to the surface for a clean W(001). Φ denotes the work function.

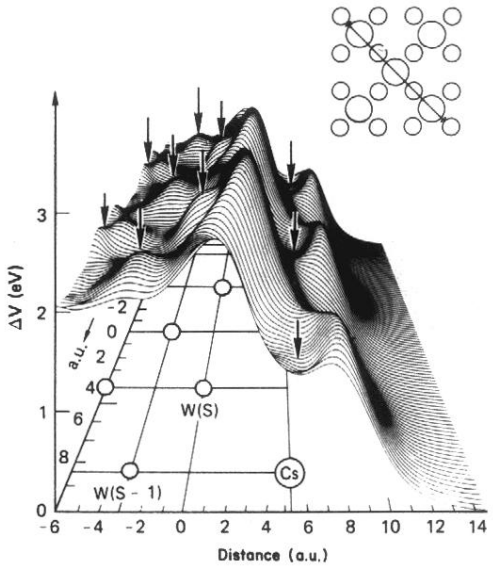

FIG. 18. Electrostatic Coulomb potential barrier originating from the polarizations in a $c(2\times2)$ Cs overlayer ($d=2.60$ Å) on a W(001) surface (corresponding to the charge redistribution shown in Fig. 13) in the (110) plane perpendicular to the surface as indicated by the inset in the upper right corner.

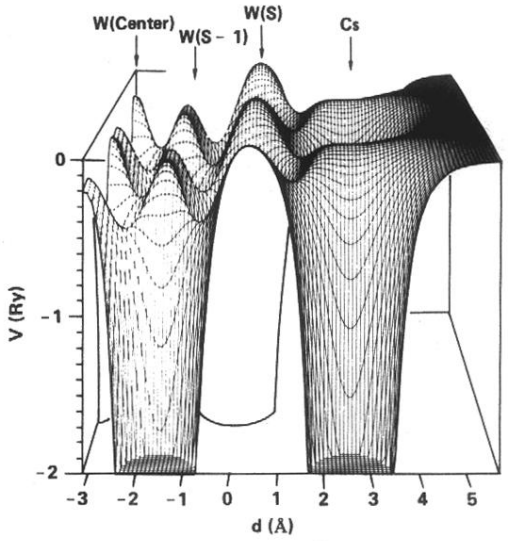

FIG. 19. Coulomb potential for $c(2\times2)$ Cs on W(001) ($d=2.60$ Å) in the (110) plane perpendicular to the surface.

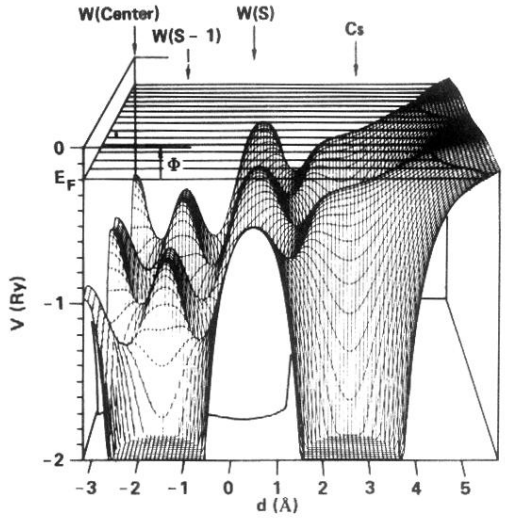

FIG. 20. Effective one-electron potential for $c(2\times2)$ Cs on W(001) ($d=2.60$ Å) in the (110) plane perpendicular to the surface. Φ denotes the work function of this system.

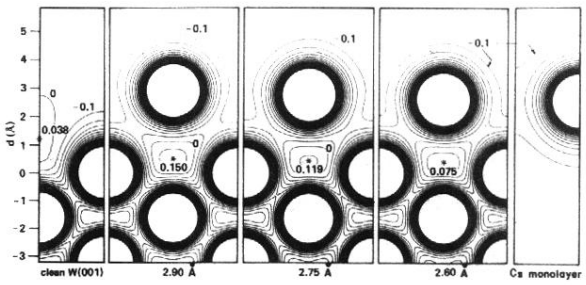

FIG. 21. Coulomb potential for a clean W(001) five-layer slab (left panel) and $c(2\times2)$ Cs on the W(001) slab for Cs heights of 2.60, 2.75, and 2.90 Å (central panels) in the (110) plane perpendicular to the surface. The Coulomb potential for the Cs monolayer is shown in the right panel.

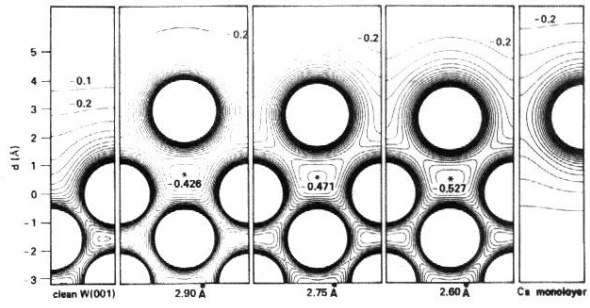

FIG. 22. Effective one-electron potential for a clean W(001) five-layer slab (left panel) and $c(2\times2)$ Cs on the W(001) slab for Cs heights of 2.60, 2.75, and 2.90 Å (central panels) in the (110) plane perpendicular to the surface. The effective potential for the Cs monolayer is shown in the right panel.

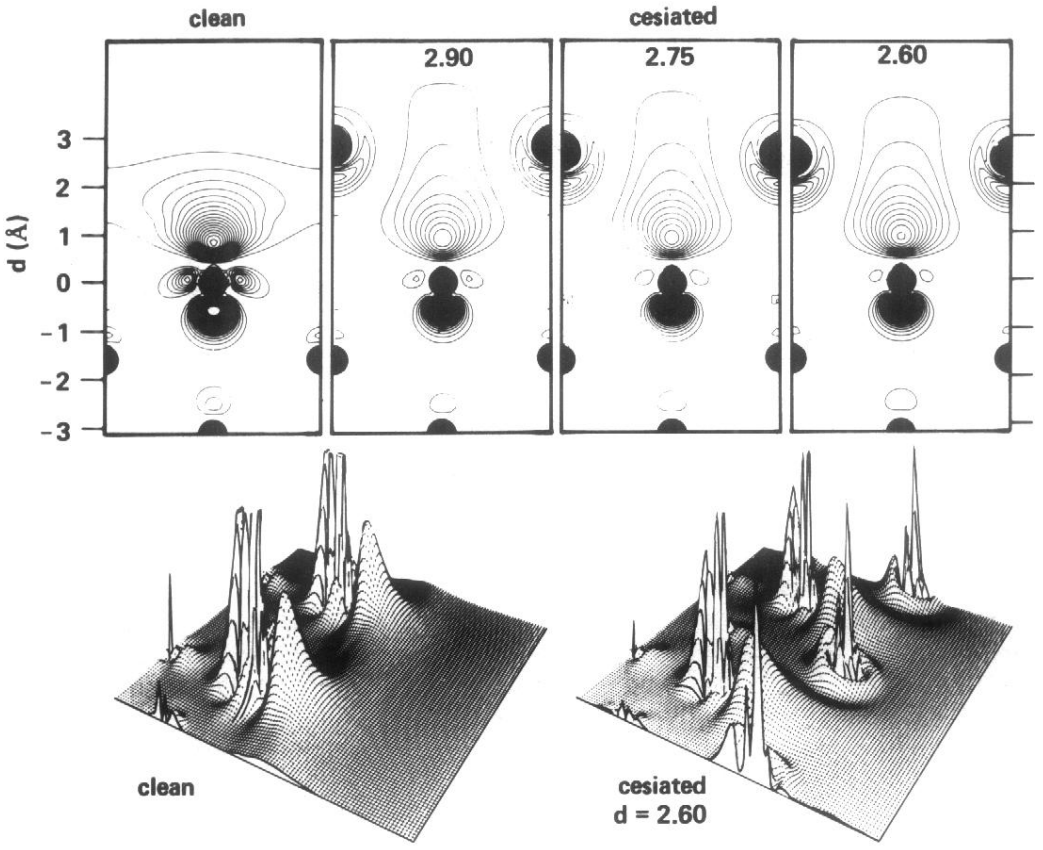

FIG. 7. Single-particle density of the adsorption-sensitive SS $\bar{\Gamma}_1$. The lowest contour and the contour spacings are 0.001 e/bohr^3. In the 3D plots shown below the cutoff is at a density of 0.030 e/bohr^3.

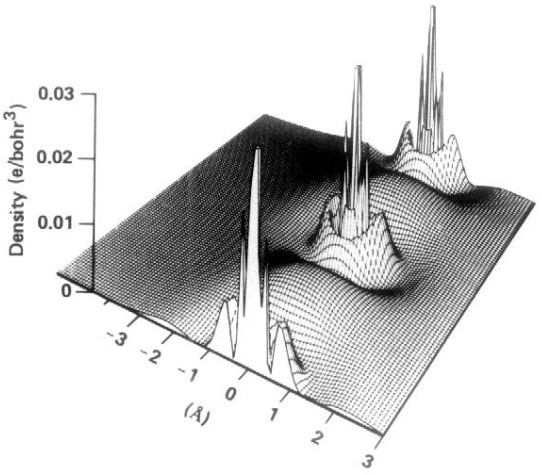

FIG. 8. Single-particle density of the $\bar{\Gamma}_1$ state at the bottom of the conduction band for a Cs monolayer. The density is given in units of e/bohr^3.

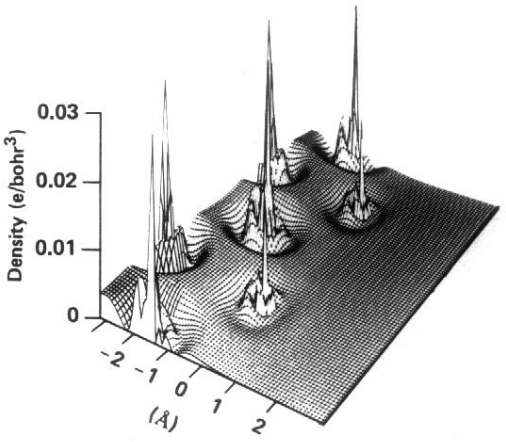

FIG. 9. Single-particle density of the $\bar{\Gamma}_1$ state at the bottom of the conduction band of the clean W(001) five-layer slab in units of e/bohr^3.